Active Offline Policy Selection

Ksenia Konyushkova[*]
DeepMind
kksenia@deepmind.com

Yutian Chen[*]
DeepMind
yutianc@deepmind.com

Tom Le Paine
DeepMind
tpaine@deepmind.com

Caglar Gulcehre
DeepMind
caglarg@deepmind.com

Cosmin Paduraru
DeepMind
paduraru@deepmind.com

Daniel J Mankowitz
DeepMind
dmankowitz@deepmind.com

Misha Denil
DeepMind
mdenil@deepmind.com

Nando de Freitas
DeepMind
nandodefreitas@deepmind.com

Abstract

This paper addresses the problem of policy selection in domains with abundant logged data, but with a restricted interaction budget. Solving this problem would enable safe evaluation and deployment of offline reinforcement learning policies in industry, robotics, and recommendation domains among others. Several off-policy evaluation (OPE) techniques have been proposed to assess the value of policies using only logged data. However, there is still a big gap between the evaluation by OPE and the full online evaluation. Yet, large amounts of online interactions are often not possible in practice. To overcome this problem, we introduce *active offline policy selection* — a novel sequential decision approach that combines logged data with online interaction to identify the best policy. We use OPE estimates to warm start the online evaluation. Then, in order to utilize the limited environment interactions wisely we decide which policy to evaluate next based on a Bayesian optimization method with a kernel that represents policy similarity. We use multiple benchmarks, including real-world robotics, with a large number of candidate policies to show that the proposed approach improves upon state-of-the-art OPE estimates and pure online policy evaluation [2].

1 Introduction

Reinforcement learning (RL) has recently proven to be successful in a range of applications from computer and board games [47, 56, 59] to robotics and chip design [38, 10, 46]. However, many challenges of real-world systems still prevent RL from being applied at scale in practice [16]. One of the limiting factors in real applications is that environment interactions are often expensive. Thus, training and evaluating agents becomes prohibitively slow and costly. Offline RL attempts to address this problem by training agents on a dataset without environment interactions [2, 23]. This enables researchers to train policies with multiple algorithms and different hyperparameter settings [51] on a single dataset. The best policy can then be chosen with off-policy policy evaluation (OPE) approaches [54, 41] (Fig. 1, left). These techniques attempt to estimate the expected agent performance by relying on the same pre-recorded dataset [28, 42, 36, 73].

---

[*]equal contribution

[2]The paper website is at https://sites.google.com/corp/view/active-ops and the code is at https://github.com/deepmind/active_ops.
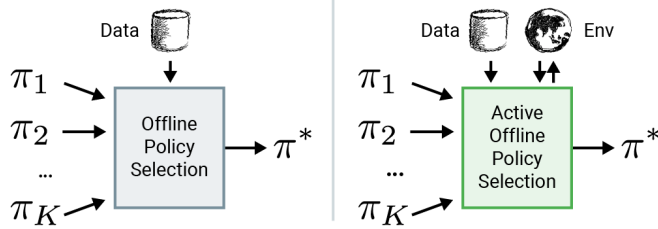
Figure 1: Left: Offline policy selection attempts to choose the best policy from a set of policies, given only a dataset of logged experiences. Right: *Active offline policy selection* additionally assumes a restricted environment interaction budget which is assigned intelligently to evaluate the most promising policies.

Unfortunately, OPE estimates are not yet precise enough to be relied upon for choosing which agent to deploy. Moreover, OPE is intrinsically limited by the pre-recorded dataset: When there is a distribution shift between a trained policy and a behavioural policy, *i.e.*, when the trained policy behaves very differently from the data collection policy, OPE is imprecise [39]. In many applications, however, a subset of policies can be evaluated *online* prior to final deployment [23, 19], even though this process can be hard and laborious. For example, in robotics a small subset of offline RL policies can be tested on the real hardware. Another example is recommender systems, which allow for restricted policy evaluation via A/B tests on a small fraction of user traffic.

In this paper, we introduce the *active offline policy selection* problem. The goal is to identify the best policy where we benefit from both offline evaluation with logged data and online evaluation with limited interaction (Fig. 1, right). In our approach we advance a solution based on Bayesian optimization (BO). It entails learning a Gaussian process (GP) surrogate function that maps policies to their expected returns. Then, we build on the GP statistics to construct an acquisition function to decide which policy to test next. To make BO successful in this problem setting, our approach has two key features. First, we incorporate existing OPE estimates as additional noisy observations (Fig. 2). This allows us to warm start online policy evaluation and to overcome the difficulties of GP hyper-parameter optimisation at the start. Second, we model correlation between policies through a kernel function based on actions that the policies take in the same states of the environment (Fig. 3). This makes our method data efficient [26] as the information about the performance of one policy informs us about the performance of similar behaving policies without costly execution in the environment. It is particularly valuable when the number of candidate policies is large (or even larger than the interaction budget).

The contributions of this paper are as follows.

1. We introduce the *active offline policy selection* problem. This problem is important in practice, but so far it has not been studied in the literature to the best of our knowledge.

2. We build a BO solution with an extended observation model to integrate both OPE estimates and interaction data. The use of OPE estimates enables us to warm-start learning a GP.

3. We propose a novel GP kernel to capture the dependency between the policies through the actions that they take. As a result, our method infers the value of one policy from those of similar policies.

The rest of this paper is organized as follows. Section 1.1 gives background on offline policy evaluation and selection. In section 2, we propose a GP model for policy value estimation, explain how we approach the sequential decision making with BO and introduce a novel kernel based on the similarity of policy outputs. Section 3 discusses the related work. Section 4 shows that active policy evaluation can improve upon the OPE after merely a few interactions, thanks to the kernel that ensures data-efficiency. Additionally, our method works reliably with OPEs of varying quality and it scales well with the growing number of candidate policies. Finally, we demonstrate our method to be efficient in the application of real-world robotics. The paper is concluded with a discussion in section 5.

1.1 Off-policy policy evaluation and selection

We consider a Markov decision process (MDP) defined by a tuple $(S, A, T, R, d_0, \gamma)$, with state space S, action space A, transition distribution $T(s'|s, a)$, reward function $R(s, a)$, initial state distribution $d_0(s)$, and discount factor $\gamma \in [0, 1]$. A policy $\pi(a|s)$ maps from S to A. The value of a policy π is measured by the expected sum of discounted rewards:

$$\mu_\pi = \mathbb{E}\left[\sum_{t=0}^{\infty} \gamma^t R(s_t, a_t)\right], \text{ with } s_0 \sim d_0(\cdot), a_t \sim \pi(\cdot|s_t), s_{t+1} \sim T(\cdot|s_t, a_t). \tag{1}$$

Typically, estimating the value of a given policy requires executing the policy in the environment many times. However, practical constraints make it difficult to run many policies of unknown quality in the environment. To address this, OPE estimates a value $\hat{\mu}_\pi$ using a dataset of trajectories $\mathcal{D}$ collected by a separate behavior policy π_β. In offline policy selection (OPS) the task is to select the policy with the highest value from a set of policies $\pi_1, \pi_2, \ldots, \pi_K$ given access only to a dataset $\mathcal{D}$ (Fig. 1, left). A straightforward approach is to select the policy with the highest OPE estimate $\hat{\mu}_{\pi_1}, \ldots, \hat{\mu}_{\pi_K}$ [20], and alternative approaches can be used depending on the quality metric [72].

2 Active offline policy selection

2.1 Problem definition

We now formally define the active offline policy selection problem. Suppose we are given a set of K candidate policies $\pi_k, 1 \le k \le K$. Denote by μ_k the unknown policy value and by ρ_k an OPE estimate computed from an offline dataset. At every step i, we can choose a policy k_i to execute in the environment once and observe the trajectory with (discounted) episodic return r_i, which is a noisy sample of the true policy value: $\mathbb{E}[r_i] = \mu_{k_i}$. We would like to find the policy with the highest value, $k^* = \arg\max_k \mu_k$, with as few trajectories (budget) as possible. Policy selection algorithm estimates the mean as m_k and recommends a policy that maximizes it: $\hat{k} = \arg\max_k m_k$. Simple regret of the recommended policy measures how close we are to the best policy:

$$\text{regret} = \mu_{k^*} - \mu_{\hat{k}}. \tag{2}$$

To solve this sequential decision problem, we introduce a GP over the policy returns and OPE estimates (subsection 2.2), and design the GP kernel over policies to model their correlated returns (subsection 2.3). Then we use these as part of a BO strategy (subsection 2.4).

2.2 Gaussian process over policy values

Given a limited interaction budget and a large number of policies, it is impossible to obtain accurate estimates of their values by executing them many times. Fortunately, similar policies tend to have similar values. Thus, propagating the information between them helps to improve the value prediction. Intuitively, the number of policies that we need to execute to find a good policy should depend on their diversity instead of the total number of candidate policies (see experiments supporting this in Fig. 8). Formally, we use GP to predict a joint distribution over the policy values.

A GP is a stochastic process, that is an indexed collection of random variables, such that every finite collection of them has a multivariate normal distribution [55]. In our case, we assume that the policy value μ as a function of policy π follows a GP, with a kernel function $\mathcal{K}(\pi_i, \pi_j)$ over policies and mean m. Specifically, we consider the following generative process for the latent policy value $\mu(\pi)$, OPE estimate ρ, and episodic return r:

$$\mu(\pi) \sim \text{GP}(m(\cdot), \mathcal{K}(\cdot, \cdot)), \quad \rho \sim \mathcal{N}(\mu(\pi), \sigma_\rho^2), \quad r \sim \mathcal{N}(\mu(\pi), \sigma_r^2). \tag{3}$$

We use a constant mean m without loss of generality. We assume a flat prior for the hyper-parameter m, and weakly informative inverse Gamma prior for the variance σ_ρ^2 and σ_r^2. Our probabilistic model is illustrated in Fig. 2.

As we have a finite number of policies, the input space is a finite set $\mathcal{X} = \{\pi_1, \ldots, \pi_K\}$, where each index corresponds to a candidate policy. The joint distribution of the K policy values reduces to a multivariate normal distribution,

$$\mu_1, \ldots, \mu_K \sim \mathcal{N}(m\mathbf{1}_K, \mathbf{K}), \text{ with } \mathbf{K}_{k,k'} = \mathcal{K}(\pi_k, \pi_{k'}), \tag{4}$$
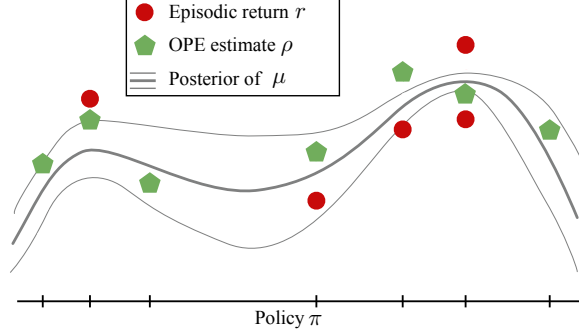
Figure 2: Gaussian process of the policy value function. We observe OPE estimates for all policies and noisy episodic returns for some of them. Neighboring policies (measured by kernel $\mathcal{K}$) have similar values, and the posterior variance is lower where there are more observations. Policies are aligned in 1D for visualization purposes, but in practice they reside in a high dimensional space.
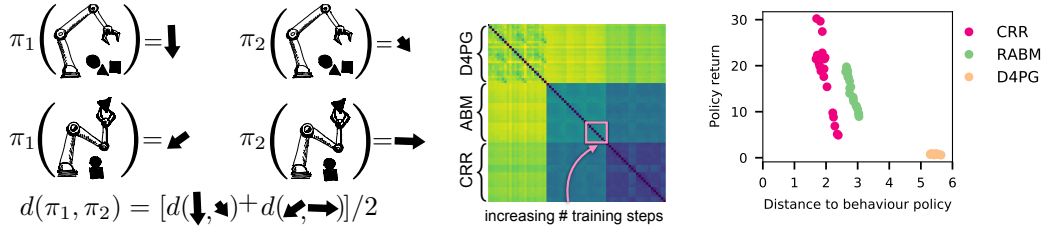

Figure 3: Left: The distance between two policies π_1 and π_2 is computed as an average distance across pairs of action vectors that are selected by each policy on a set of states. Middle: Pairwise distance matrix between policies on `humanoid-run` task. High distance is shown in yellow and low distance in dark blue. The 3×3 block structure of the matrix reflects the 3 types of training algorithm. Smaller blocks correspond to the increasing number of training steps with the same hyperparameters. Right: Policy value (μ_π) versus action distance to the behavior policy $\bar{d}(\pi, \pi_\beta)$. Policies with the same training algorithm are in the same color.

where $\mathbf{1}_K$ is a K-length vector of ones. For each policy π_k, we have one noisy observation from an OPE method ρ_k, and zero or multiple noisy episodic return observations r_k^i. As the policies are related through the covariance matrix $\mathbf{K}$, observing a return sample from one policy updates the posterior distribution of all of them. Given the OPE estimates $\boldsymbol{\rho} = [\rho_1, \ldots, \rho_K]$ and N_k return observations $\mathbf{r}_k = [r_k^1, \ldots, r_k^{N_k}]$ for each policy π_k, the posterior distribution of the mean return is also a Gaussian,

$$\mu_1, \ldots, \mu_K | \boldsymbol{\rho}, \{\mathbf{r}_k\}_k \sim \mathcal{N}(\mathbf{m}, \boldsymbol{\Sigma}), \text{ with}$$

$$\mathbf{m} = \mathbf{K}(\mathbf{K} + \boldsymbol{\Lambda})^{-1}\mathbf{y}, \qquad \boldsymbol{\Sigma} = \mathbf{K} - \mathbf{K}(\mathbf{K} + \boldsymbol{\Lambda})^{-1}\mathbf{K}.$$

$$\mathbf{y}_k = \left(\frac{1}{\sigma_\rho^2} + \frac{N_k}{\sigma_r^2}\right)^{-1}\left(\frac{\rho_k}{\sigma_\rho^2} + \frac{1}{\sigma_r^2}\sum_{i=1}^{N_k} r_k^i\right), \qquad \boldsymbol{\Lambda}_{kk} = \left(\frac{1}{\sigma_\rho^2} + \frac{N_k}{\sigma_r^2}\right)^{-1}, \qquad (5)$$

where $\boldsymbol{\Lambda}$ is a diagonal matrix with diagonal entries defined above.

2.3 Kernel

A key component of the GP model is the kernel that measures our belief about the policy correlation. To obtain a kernel we make a key assumption: *Policies that are similar in the actions that they take, yield similar returns*. Then, our insight is to measure the distance between the policies through the actions that each of them takes on a fixed set of states from the offline dataset (Fig. 3, left).

Formally, to measure the similarity between π_1 and π_2, we obtain the policy actions at a given state s and measure the distance between these two action vectors $d(\pi_1(s), \pi_2(s))$ [3]. We then define the

---

[3]In this work, we use Euclidean distance for deterministic policies with continuous actions and Hamming distance for discrete actions. An extension to stochastic policies is straightforward.

distance between the two policies as the average distance over the states of the offline dataset $\mathcal{D}$,

$$\bar{d}(\pi_1, \pi_2) = \mathbb{E}_{s \sim \mathcal{D}} \, d(\pi_1(s), \pi_2(s)) \, . \tag{6}$$

In practice we approximate $\bar{d}$ using a randomly sampled subset of states $\mathcal{D}' \subset \mathcal{D}$.

An example of a pairwise distance matrix for a set of policies is shown in Fig. 3, middle. Rows and columns are the policies which are arranged first by the type of the training algorithm, then by hyperparameters and finally by the training steps (none of which is observed by our method). Note the block structure, which reflects the different nature of training algorithms. Smaller blocks of increasing policy distances correspond to policies with more training steps and the same hyperparameters.

Additionally, Fig. 3, right shows an example of policy distances to the behaviour policy. The values of policies produced by the same algorithm change gradually as a function of this distance. It provides indication that our kernel construction is informative for predicting the value of a policy.

Finally, we compute Matérn 1/2 kernel as: $\mathcal{K}(\pi_1, \pi_2) = \sigma_k^2 \exp(-\bar{d}(\pi_1, \pi_2)/l)$, where σ and l are the trainable variance and length-scale hyperparameters. This is a popular kernel choice [57]. As the distance metric is the average distance over states, using it in this kernel is equivalent to multiplication of kernels on these states and it is a valid positive semi-definite matrix.

2.4 Active offline policy selection with Bayesian optimization

Under a GP formulation, we can employ BO [57] to search for the best policy efficiently. BO optimizes an unknown function $\mu(\pi)$ with $\pi \in \mathcal{X}$ using a limited number of function queries that render noisy observations. BO has been used successfully in many applications including experimental design [5], robotics [43, 44], hyper-parameter optimization [60, 27, 12], preference learning and interactive machine learning [9, 8]. The key component of a BO algorithm is an acquisition function $u_i(\pi)$ that balances exploration and exploitation when selecting a query. Widely used acquisition functions include upper confidence bounds (UCB), expected improvement (EI) and epsilon-greedy. Here, we simply use the UCB acquisition function [61, 30].[4] Specifically, at every step i, we compute the score for a policy π_k using

$$u_i(k) = \mathbf{m}_k + \sqrt{\beta_i \mathbf{\Sigma}_{kk}}, \tag{7}$$

where β_i is a constant depending on i. We then choose the policy with the highest score, $k_i = \arg \max_k u_i(k)$, to execute next. After observing a new return r_{k_i}, we update $\mathbf{m}$ and $\mathbf{\Sigma}$ in Eq. 5. We also update the hyper-parameters (m, σ_ρ^2, σ_r^2, σ_k^2 and l) with the maximum a posteriori estimate (see details in the appendix).

Estimating the hyper-parameters with limited data is challenging in practice. Fortunately, in the active offline policy selection formulation, we can take advantage of the OPE estimates as prior observations to fit the hyper-parameters before launching the interactive optimization process. In some ablations where OPE is not available we instead execute 5 randomly sampled policies before fitting the hyperparameters.

3 Related work

Offline RL becomes increasingly popular due to its ability to leverage offline data to learn policies for RL in the real world. As a results, several benchmark datasets were recently announced [23, 19]. Offline RL methods include policy-constraint approaches that regularize the learned policy to stay close to the behavior policy [71, 21], value-based approaches that encourage more conservative estimates, either through regularization or uncertainty [35, 22], model-based approaches [74, 31], and standard RL methods used in off-policy RL [7].

OPE is studied extensively across many domains [40, 67, 29, 50]. It includes methods that use importance sampling [53] or stationary state distribution [42, 49, 68], value function [64, 45, 65], or learned transition models [75], as well as methods that combine these approaches [48, 15, 28, 18]. OPS is a related practical problem that receives increasing interest [51, 72, 20]. Our work has two notable distinctions in contrast to these prior works: 1) we consider similarities between policies when

---

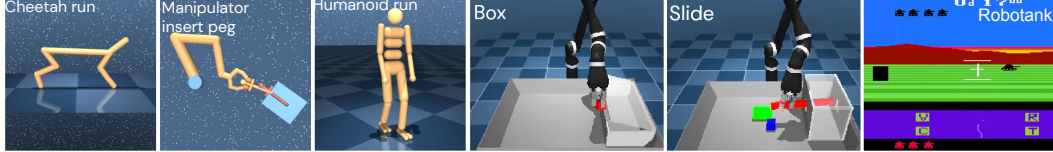[4]Experiments with other acquisition functions can be found in the supplementary materials.

Figure 4: Environment used in the experiments. 9 environments from the dm-control domain (3 examples on the left), 4 from the MPG domain (2 examples in the middle), and 3 from Atari domain (1 example on the right).

making value predictions, and 2) we focus on active setting, where a small number of evaluations in the environment can help to quickly improve the prediction of the best policy.

Similar to the way the kernel is computed based on policy's actions, Policy Evaluation Networks [24] work considers a network fingerprinting that learns a policy embedding through the outputs of the policy on probing states. The principal difference to our approach is that we only consider a very limited online policy evaluation budget (in the order of 100) while network fingerprinting needs many policy evaluations to train the policy embeddings (in the order of $100\,000$).

Applying BO in a finite set of indices reduces the problem to a Bayesian multiarmed bandit problem. Exploring the shared structure among arms using Bayesian models has been studied in the literature [61, 33, 26]. Our work builds upon the Bayesian bandit model to address the problem of policy selection additionally exploiting the offline dataset.

Active learning is used in RL for better exploration, learning reward or world models [17, 3, 14, 34, 6]. It has not been studied for the OPE or OPS problems to the best of our knowledge. Related to the policy representation through actions in the kernel, classifiers in active learning can be also characterised by their predictions on a subset of datapoints [32]. Furthermore, diversity in policies was measured through the action distribution for sampled states in population-based setting [52].

4 Experiments

4.1 Datasets and environments

In our experiments we consider three domains (Fig. 4) with different properties. Two domains are standard benchmarks in RL for continuous and discrete control and another one is motivated by the challenges of evaluating control policies in robotics. For each domain we describe the environments, datasets for offline RL and OPE, and sets of policies below. More details are provided in Appendix B.

DeepMind Control Suite (dm-control)   This is a standard set of continuous control environments [66]. It contains 9 tasks of locomotion and manipulation, some of which are shown in Fig. 4, left. The observations are the state of the MPD, including joint angles and velocities. The dimensionality and semantics of the continuous actions vary across tasks. We use the offline RL policies from DOPE [20] (a benchmark for OPE and OPS) that are trained using the dataset from the RL Unplugged benchmark [23]. For each task, there are up to 96 policies with various algorithms (D4PG [7], ABM [58], and CRR [71]), hyperparameters, and number of training steps.

Manipulation Playground (MPG)   This is a simulated robotics environment. The task is to control a Kinova Jaco arm with 9 degrees of freedom. Joint velocity control of 6 arm and 3 hand joints is used. The policies are learnt from proprioception and image input from frontal and in-hand cameras of 64×64 dimensions. We perform 4 manipulation tasks within a 20×20 cm basket (Fig. 4, middle). The dataset is generated by running an online RL algorithm as in [71] and the policies are generated as in [51]. For each task, there are up to 256 policies trained with various algorithms (including BC, D4PG [7], and CRR [71]), and hyperparameters.

Atari   This is a popular benchmark with discrete actions in online and offline RL [23]. For each of 3 games we trained 210 policies on an offline dataset [23] from high dimensional pixel observations with six offline RL methods, including Double DQN [69], CQL [35], BCQ [21], REM [2] and BVE [22]. As the range of returns is quite different from the other two domains, we scale the discounted returns to have approximately the same mean and variance based on the offline RL dataset.
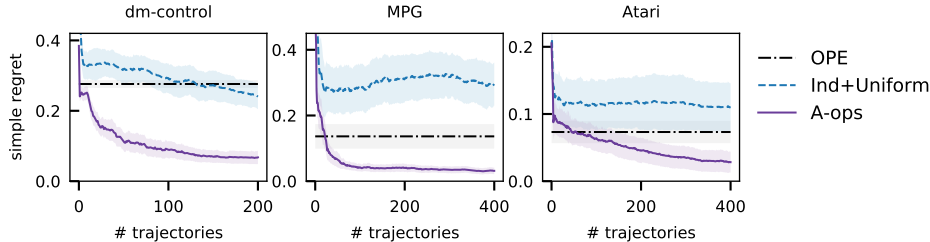
Figure 5: Comparison of A-OPS approach, offline policy selection with OPE, and online policy selection with IND+UNIFORM on dm-control, MPG and Atari environments. The results are averaged across 9, 4 and 3 tasks and 100 experiments in each of them. Shaded areas show standard deviation of the mean. Our method A-OPS quickly surpasses the baselines and achieves the lowest regrets.

We obtain OPE estimates for each policy by running Fitted Q-Evaluation (FQE) [45, 36] on the offline RL data. FQE is the default OPE method used in our experiments unless stated otherwise.

4.2 Experimental setting and implementation

To evaluate the policy selection procedure in each experiment we randomly select a subset of K policies out of all trained policies. We set $K = 50$ for dm-control and $K = 200$ for MPG and Atari. Then, we repeat each experiment 100 times, and report the average results and the standard deviation of the mean estimate. As a performance metric we monitor the simple regret (Eq. 2) as a function of the number of executed episodes. The algorithms are progressively evaluated when each trajectory is added. To make the results comparable across domains, we first compute the gap between the best and the worst performing policy in each environment across all the policies. Then, we normalise the scores in each experiment by dividing them by this gap. The results by environment are discussed in the appendix.

Independent policy model   To study the contribution of modeling the policy correlation with GP, we consider a baseline model with independently distributed value μ_k across policies. The data generating process for the k-th policy follows a hierarchical Gaussian distribution:

$$r_k^i \overset{iid}{\sim} \mathcal{N}(\mu_k, \sigma_{k,r}^2), \forall i, \text{ with } \mu_k \sim \mathcal{N}(\rho_k, \sigma_{k,\rho}^2), \tag{8}$$

where we assume a weakly informative inverse Gamma prior for variance $\sigma_{k,r}^2$ and $\sigma_{k,\rho}^2$ as in GP. We refer to this model as independent policy model (IND). Such model can be used in combination with any policy sampling strategy.

All online and offline RL algorithms, as well as offline policy evaluation algorithms in this work are implemented with Acme [25] and Reverb [11], and run on GPUs on an internal cluster. We implement GP and IND together with all BO algorithms using the same TensorFlow [1] codebase, and run all the policy selection experiments using CPUs. Details about the tasks and policies, hyperparameter values, and additional BO algorithms and ablations are presented in the appendix.

4.3 Comparison to the existing methods

In our main experiments we would like to verify that the proposed method performs better than two strategies commonly employed in practice (see section 1). To this end, we compare:

1. **A-OPS**: Active-Offline Policy Selection, our proposed method that uses OPE estimates to bootstrap GP learning and performs UCB policy sampling as discussed in section 2.
2. **OPE**: standard offline policy selection technique that selects the policy with the highest OPE estimate [51].
3. **IND+UNIFORM**: standard online selection where we execute policies uniformly and select the one with the highest return belief (estimated with independent policy model IND).

Fig. 5 presents the simple regret as a function of the number of executed trajectories. The results are averaged across 9 tasks from dm-control, 4 tasks from MPG and 3 games from Atari. Our

7

	No OPE		With OPE	
	Independent	**GP**	**Independent**	**GP**
Uniform	IND+UNIFORM	GP+UNIFORM	IND+UNIFORM+OPE	GP+UNIFORM+OPE
UCB	IND+UCB	GP+UCB	IND+UCB+OPE	A-OPS

Table 1: Design of the ablation experiments across three axes: the use of OPE, GP or independent policy model, active policy selection or uniform sampling. We refer to our method that combines all the components as A-OPS.
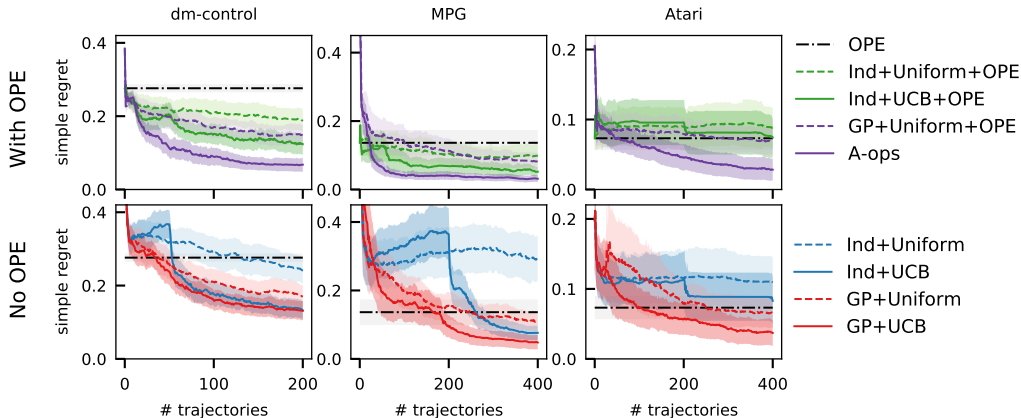

Figure 6: Ablations. In three domains, we ablate each of three components of our approach. 1) The use of OPE (with OPE in the first row and without in the second). 2) The choice of policy model: GP (purple and red) and independent (green and blue). 3) The policy selection strategy: active (dark, solid line) and uniform sampling (lighter, dashed line). In general, active is better than uniform, methods that exploit policy correlation are better than methods that do not, and methods that use an OPE prior are better than those that do not.

proposed method A-OPS combines offline and online policy evaluations. It quickly outperforms OPE and improves with more trajectories. A-OPS estimate of the best policy may be erroneous initially due to noisy reward samples (*e.g.*, in MPG), but it quickly updates, thus allowing for significant improvements over OPE only after a few actively selected trajectories.

When comparing offline and online policy selection we notice that for the range of considered budgets, online policy selection IND+UNIFORM performs worse than OPE. It suggests that single trajectory returns are noisier than OPE estimates in these environments (more discussion on this is in the appendix). Naturally, we expect that given a larger budget the online baseline will eventually surpass its offline counterpart in all domains.

4.4 Component ablations

We are not aware of other works on active offline policy selection. Thus, in this section we investigate alternative solutions that help us to understand the importance of the proposed components of A-OPS. We design our ablation studies to test the contribution of the three components of A-OPS:

1) *OPE*: initialisation of algorithms with or without OPE estimates.
2) *active learning*: active policy selection (UCB) or uniform sampling (UNIFORM).
3) *policy kernel*: GP model or independent model baseline (IND).

Tab. 1 summarises the 8 possible combinations of the components. We refer to our full method (GP+UCB+OPE) simply as A-OPS. We also include the pure offline OPE estimates as before.

The results with all the baselines in two domains are presented in Fig. 6. First of all we observe that A-OPS outperforms all other methods across a wide range of budgets, thus, all the components are crucial for the performance of our method and excluding any of them leads to significantly worse results. Next, we answer three questions about each component individually.

1. How important is it to incorporate OPE estimates? Across all the experiments, incorporating OPE estimates (top row of Fig. 6) always considerably improves the results compared to starting policy selection from scratch (bottom row). For example, in MPG when A-OPS starts with OPE, it is able to cut the OPE regret by more than half before executing 100 trajectories. For this budget, GP+UCB, which starts from scratch, does not reach the same regret as OPE.

2. How informative is our kernel? To understand the value of modelling the correlation between policies through the kernel, we compare the GP method with the independent policy model (IND). In Fig. 6 purple and red lines use GP as the policy model and green and blue use the IND model. In the vast majority of settings (11 out of 12) the use of a kernel significantly improves the results and in one setting (IND+UNIFORM+OPE vs GP+UNIFORM+OPE in MPG domain) they perform on par. We conclude that the kernel is a key ingredient for improving data efficiency.

3. How important is the selection strategy? The active selection of policies is generally beneficial for identifying a good policy. For this we refer to the results of dashed lines that correspond to UNIFORM policy selection and solid lines that correspond to the use of UCB. Using IND+UCB yields a high regret in the initial exploration stage, but it improves substantially over IND+UNIFORM later. Moreover, incorporating OPE estimates and a kernel (resulting in A-OPS) significantly shortens the exploration stage.

4.5 Results on the real robot

Evaluation of the offline RL policies is a bottleneck in real world robotic applications because robotic resources are limited and robots cannot be accelerated beyond real time. Thus, we believe it is important to carefully design the evaluation procedure. Here we consider a robotic stacking task, where we train a single policy to operate a robotic arm to stack different object groups, each group containing objects of diverse shapes. It receives a reward of 1 if the stacking goal is achieved in that step. See [37] for detailed task description. In our experiments we propose to use A-OPS method components in two ways: for selecting the best policy among a set and for selecting the best snapshot of a policy.

Selecting the best policy We use 36 real robot policies from [37] (skill mastery, Tab. 2, 3). Here we treat all 5 object groups together as one evaluate setting and one policy evaluation is equivalent to running the policy to generate one stacking trajectory for each group. The policies are trained with either a sim2real and offline RL approach, both of which do not involve direct interactions with the physical robot. We measure the cumulative discounted return to be consistent with the rest of the experiments, while in [37] binary success is used. For the kernel, we normalise each action dimension by its variance, but the rest of the settings and hyperparameters is consistent with simulated experiments. In each experiment we select 20 out of 36 policies. The results are reported in Fig. 7.

In Fig. 7, left we compare A-OPS to the strategies that are commonly used in practice: pure online evaluation (IND+UNIFORM) and pure offline evaluation with OPE. There is a large variance in returns obtained by a single policy and as a result IND+UNIFORM reduces the regret slowly. The OPE method of our choice (FQE) ranks policies very well (see Appendix F) and its regret is very low. However, after less than 200 policy evaluations, A-OPS is able to achieve even lower simple regret. The full ablations are presented in Fig. 7, middle (strategies which use OPE) and right (strategies without OPE). The full A-OPS approach outperforms the other alternatives but the variance of the results is high.

Selecting the best snapshot The Gaussian process that is at the core of A-OPS could be also used for selecting the best checkpoint which is equivalent to deciding on the number of training steps for the policy. In our experiment, we consider 69 checkpoints of the best performing policy from [37]. Then, we use the results of full policy evaluation of 36 policies and make predictions for all the checkpoints. We select 5 most promising checkpoints and send them for evaluation on the real robot. The evaluation results are presented in Tab. 2. We show the return for a given number of training steps for the evaluated checkpoints and the existing best policy (shown in blue). All selected checkpoints slightly improve the results compared to the previous best agent and the improvements are between 1.55% and 4.95%, we highlight the best checkpoint in bold. We conclude that the proposed methodology might be useful for the task of deciding on the number of training steps.
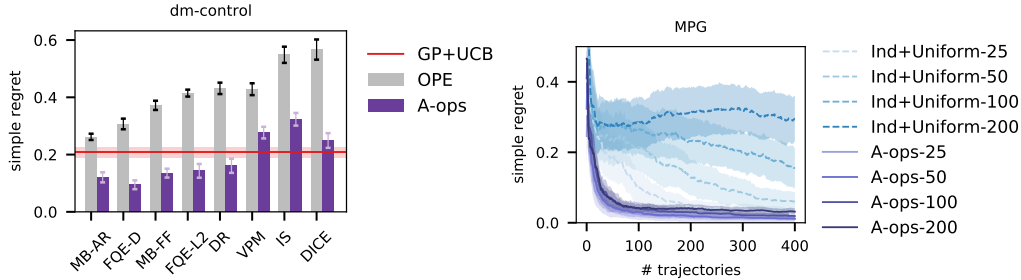
Figure 8: Left: The performance of A-OPS on dm-control with varying type of OPE estimate with a budget of 50 trajectories. The various OPE methods are Model-Based OPE with an auto-regressive transition model (MB-AR), Fitted Q Evaluation with distributional Q function and distributional loss (FQE-D), Model-Based OPE with a feedforward transition model (MB-FF), Fitted Q Evaluation with standard Q function and L2 loss (FQE-L2), Double Robust (DR), Variational Power Method (VPM), Importance Sampling (IS), Distribution Correction Estimation (DICE). A-OPS can improve upon the initial OPE estimates in all cases. Right: Performance of A-OPS and IND+UNIFORM with varying number of policies available for execution. IND+UNIFORM is affected a lot by the increase in the number of policies. Our approach A-OPS performs similarly when the number of policies is increase by a factor of almost 10.

training step	discounted return
841 000	25.58
983 000	**25.81**
1 143 000	25.33
1 283 000	25.07
1 303 000	24.98
1 003 000	24.59

Table 2: The best current policy is shown in blue, the newly discovered best policy is in **bold**. A-OPS components is promising for identifying the best checkpoint.
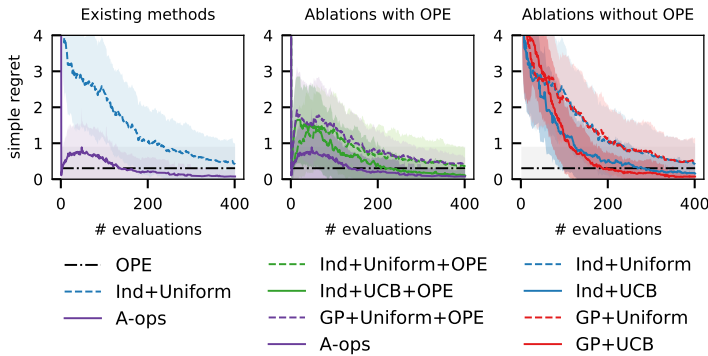
Figure 7: A-OPS results on the real robot. The comparison of A-OPS with the commonly used strategies is shown on the left, ablations when using OPE is in the middle and without OPE is on the right. A-OPS is able to reach the best simple regret with a moderate evaluation budget.

4.6 More ablation studies

Incorporating the OPE estimates is clearly beneficial for policy selection. Here, we further study: **How does the performance depend on the quality of OPE estimates?** Fig. 8, left compares A-OPS using estimates from different OPE algorithms in DOPE [20] on dm-control with a small budget of 50 trajectories. A-OPS always improves upon the corresponding OPE estimate, and the performance clearly depends on the quality of the associated OPE estimate. The performance of GP+UCB with 50 trajectories that does not rely on any OPE metric is shown as a horizontal line. Some OPE estimates (e.g., IS, VPM and DICE) have large estimation errors and even a negative correlation with the ranks of policies [20]. As expected, A-OPS is negatively impacted by poor OPE estimates and ignoring them could yield better results. It should be possible to correct for this to a greater extent with more online observations. For now we follow the recommendation to use the FQE estimates.

In subsection 2.2 we hypothesised that A-OPS method should be data efficient as it would scale with the diversity of policies and not their number. We next try to verify it and answer the question: **How does the policy selection algorithm scale with the growing number of candidate policies?** In Fig. 8, right we show the simple regret for A-OPS and IND+UNIFORM in the MPG domain when we sample 25, 50, 100 and 200 policies. We see that when the number of policies is not very high (25), the algorithm that treats policies independently and samples them at uniform (IND+UNIFORM-25) can closely approach the performance of our method A-OPS-25 after 100 trajectories. However, when the number of policies grows, this small interaction budget is not enough for the naive algorithm: IND+UNIFORM-200 significantly degrades its performance. At the same time, A-OPS-200 is minimally affected by the increase in the number of policies as the diversity of the policies stays approximately the same.
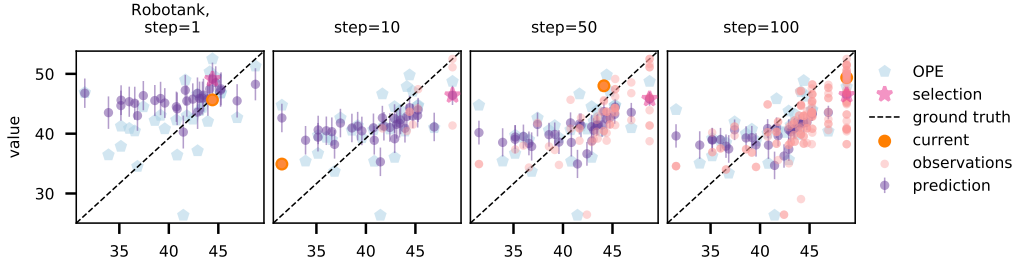
Figure 9: Visualisation of the qualitative performance of A-OPS algorithm on `Robotank` environment with 20 randomly selected policies (ordered by ground truth only for the illustration purpose). From left to right we show the state at 1, 10, 50, 100 algorithm iterations. The initial OPE scores are shown in light blue, the policy selected by A-OPS is highlighted with magenta star, the observation of the currently executed policy is shown in orange circle, past observations are in pink and the prediction with its standard deviation is in purple.

4.7 Qualitative results

Finally, to understand the behaviour of A-OPS method we show its progress for one of the experiments with Robotank game in Fig. 9. For visualisation purposes, we use only 20 policies which are ordered by their ground truth returns (not observed by the method). Perfect value predictions would be aligned along the diagonal line. We show the initial *OPE* values, current *selection* of the best policy, *current* observation of the executed policy, past *observations* and the algorithm *prediction* with its standard deviation for steps 1, 10, 50, and 100. The A-OPS prediction is determined by the OPE observations and past observations of the policy returns. The kernel reinforces smoothness of the function. We can see that the initial selection is dominated by OPE prediction and the selected policy is quite far from the best policy. With more online observations, the predictions improve. Our algorithm is data-efficient because 1) it samples more promising policies more frequently (more observations with higher scores), 2) the knowledge from one policy is propagated to the policies related by the kernel (predictions for some policies are updated without any new observations of their values).

5   Conclusions

In this paper, we introduced the active offline policy selection problem. We proposed a BO solution that integrates OPE estimates with evaluations obtained by interacting with the environment. We also designed a novel kernel that models correlation over policies. Experiments on three control domains proved that our solution is very effective. Furthermore, our experiments ablated the different components of the solution, highlighting the value of modelling correlation via the kernel, active selection, and incorporation of OPE estimates in the observation model. Finally, we have also demonstrated that our approach is efficient on the real robot.

Limitations and future work   The A-OPS approach could be of use in many safety critical applications. This work does not deal with this question explicitly as we assume safety constraints to be implemented directly on the hardware. It means that if an unsafe policy is attempted, the safety controller would terminate the policy before reaching the end of an episode, resulting in low reward and thus discouraging A-OPS from trying this policy again. Alternatively, we could alleviate this limitation by applying constrained BO techniques [63] to search for the best policy without violating safety constraints.

In this work, we explore the policy structure based on the offline dataset, and use every new trajectory only to obtain a noisy observation of policy values. This allows a clean Bayesian optimization formulation. Going forward, more information could be extracted from the new trajectories, for example, to further improve OPE estimates, GP kernel, or policies themselves. However, using this information would make the solution much more complex and we may need to take the additional computational cost into account. Finally, to construct a better policy kernel, we may investigate how to measure the policy similarity on the most informative subset of states in the offline dataset.

Acknowledgements

References

[1] Martín Abadi, Ashish Agarwal, Paul Barham, Eugene Brevdo, Zhifeng Chen, Craig Citro, Greg S. Corrado, Andy Davis, Jeffrey Dean, Matthieu Devin, et al. TensorFlow: Large-scale machine learning on heterogeneous systems, 2015. Software available from tensorflow.org.

[2] Rishabh Agarwal, Dale Schuurmans, and Mohammad Norouzi. An optimistic perspective on offline reinforcement learning. In *International Conference on Machine Learning*, 2020.

[3] Takayuki Akiyama, Hirotaka Hachiya, and Masashi Sugiyama. Efficient exploration through active learning for value function approximation in reinforcement learning. *Neural Networks*, 2010.

[4] Jean-Yves Audibert, Sébastien Bubeck, and Rémi Munos. Best arm identification in multi-armed bandits. In *Conference on Computational Learning Theory*, 2010.

[5] Javad Azimi, Ali Jalali, and Xiaoli Zhang Fern. Hybrid batch bayesian optimization. In *International Conference on Machine Learning*, 2012.

[6] Philip Ball, Jack Parker-Holder, Aldo Pacchiano, Krzysztof Choromanski, and Stephen Roberts. Ready policy one: World building through active learning. In *International Conference on Machine Learning*, 2020.

[7] Gabriel Barth-Maron, Matthew W Hoffman, David Budden, Will Dabney, Dan Horgan, TB Dhruva, Alistair Muldal, Nicolas Heess, and Timothy Lillicrap. Distributed distributional deterministic policy gradients. In *International Conference for Learning Representations*, 2018.

[8] E. Brochu, T. Brochu, and N. de Freitas. A Bayesian interactive optimization approach to procedural animation design. In *ACM SIGGRAPH/Eurographics Symposium on Computer Animation*, 2010.

[9] E. Brochu, N. de Freitas, and A. Ghosh. Active preference learning with discrete choice data. In *Advances in Neural Information Processing Systems*, 2007.

[10] Serkan Cabi, Sergio Gómez Colmenarejo, Alexander Novikov, Ksenia Konyushkova, Scott Reed, Rae Jeong, Konrad Zolna, Yusuf Aytar, David Budden, Mel Vecerik, et al. Scaling data-driven robotics with reward sketching and batch reinforcement learning. In *Robotics: Science and Systems Conference*, 2020.

[11] Albin Cassirer, Gabriel Barth-Maron, Eugene Brevdo, Sabela Ramos, Toby Boyd, Thibault Sottiaux, and Manuel Kroiss. Reverb: A framework for experience replay. *arXiv preprint arXiv:2102.04736*, 2021.

[12] Yutian Chen, Aja Huang, Ziyu Wang, Ioannis Antonoglou, Julian Schrittwieser, David Silver, and Nando de Freitas. Bayesian optimization in AlphaGo. *arXiv preprint arXiv:1812.06855*, 2018.

[13] Will Dabney, Georg Ostrovski, David Silver, and Rémi Munos. Implicit quantile networks for distributional reinforcement learning. In *International Conference on Machine Learning*, 2018.

[14] Christian Daniel, Malte Viering, Jan Metz, Oliver Kroemer, and Jan Peters. Active reward learning. In *Robotics: Science and Systems Conference*, 2014.

[15] Miroslav Dudík, John Langford, and Lihong Li. Doubly robust policy evaluation and learning. *arXiv preprint arXiv:1103.4601*, 2011.

[16] Gabriel Dulac-Arnold, Daniel J. Mankowitz, and Todd Hester. Challenges of real-world reinforcement learning. *arXiv preprint arXiv:1904.12901*, 2019.

[17] Arkady Epshteyn, Adam Vogel, and Gerald DeJong. Active reinforcement learning. In *International Conference on Machine Learning*, 2008.

[18] Mehrdad Farajtabar, Yinlam Chow, and Mohammad Ghavamzadeh. More robust doubly robust off-policy evaluation. In *International Conference on Machine Learning*, 2018.

[19] Justin Fu, Aviral Kumar, Ofir Nachum, George Tucker, and Sergey Levine. D4RL: Datasets for deep data-driven reinforcement learning. *arXiv preprint arXiv:2004.07219*, 2020.

[20] Justin Fu, Mohammad Norouzi, Ofir Nachum, George Tucker, ziyu wang, Alexander Novikov, Mengjiao Yang, Michael R Zhang, Yutian Chen, Aviral Kumar, Cosmin Paduraru, Sergey Levine, and Thomas Paine. Benchmarks for deep off-policy evaluation. In *International Conference for Learning Representations*, 2021.

[21] Scott Fujimoto, David Meger, and Doina Precup. Off-policy deep reinforcement learning without exploration. In *International Conference on Machine Learning*, 2019.

[22] Caglar Gulcehre, Sergio Gómez Colmenarejo, Ziyu Wang, Jakub Sygnowski, Thomas Paine, Konrad Zolna, Yutian Chen, Matthew Hoffman, Razvan Pascanu, and Nando de Freitas. Regularized behavior value estimation. *arXiv preprint arXiv:2103.09575*, 2021.

[23] Caglar Gulcehre, Ziyu Wang, Alexander Novikov, Tom Le Paine, Sergio Gomez Colmenarejo, Konrad Zolna, Rishabh Agarwal, Josh Merel, Daniel Mankowitz, Cosmin Paduraru, et al. RL Unplugged: A suite of benchmarks for offline reinforcement learning. *arXiv preprint arXiv:2006.13888*, 2020.

[24] Jean Harb, Tom Schaul, Doina Precup, and Pierre-Luc Bacon. Policy evaluation networks. *arXiv preprint arXiv:2002.11833*, 2020.

[25] Matt Hoffman, Bobak Shahriari, John Aslanides, Gabriel Barth-Maron, Feryal Behbahani, Tamara Norman, Abbas Abdolmaleki, Albin Cassirer, Fan Yang, Kate Baumli, et al. Acme: A research framework for distributed reinforcement learning. *arXiv preprint arXiv:2006.00979*, 2020.

[26] Matthew Hoffman, Bobak Shahriari, and Nando de Freitas. On correlation and budget constraints in model-based bandit optimization with application to automatic machine learning. In *Artificial Intelligence and Statistics*, 2014.

[27] F. Hutter, H. H. Hoos, and K. Leyton-Brown. Sequential model-based optimization for general algorithm configuration. In *Learning and Intelligent Optimization*, 2011.

[28] Nan Jiang and Lihong Li. Doubly robust off-policy value evaluation for reinforcement learning. In *International Conference on Machine Learning*, 2016.

[29] Dmitry Kalashnikov, Alex Irpan, Peter Pastor, Julian Ibarz, Alexander Herzog, Eric Jang, Deirdre Quillen, Ethan Holly, Mrinal Kalakrishnan, Vincent Vanhoucke, et al. QT-Opt: Scalable deep reinforcement learning for vision-based robotic manipulation. In *Conference on Robot Learning*, 2018.

[30] Emilie Kaufmann, Olivier Cappé, and Aurélien Garivier. On Bayesian upper confidence bounds for bandit problems. In *Artificial intelligence and statistics*, 2012.

[31] Rahul Kidambi, Aravind Rajeswaran, Praneeth Netrapalli, and Thorsten Joachims. Morel: Model-based offline reinforcement learning. *arXiv preprint arXiv:2005.05951*, 2020.

[32] Ksenia Konyushkova, Raphael Sznitman, and Pascal Fua. Discovering general-purpose active learning strategies. *arXiv preprint arXiv:1810.04114*, 2019.

[33] Andreas Krause and Cheng S Ong. Contextual gaussian process bandit optimization. *Advances in Neural Information Processing Systems*, 2012.

[34] David Krueger, Jan Leike, Owain Evans, and John Salvatier. Active reinforcement learning: Observing rewards at a cost. *arXiv preprint arXiv:2011.06709*, 2020.

[35] Aviral Kumar, Aurick Zhou, George Tucker, and Sergey Levine. Conservative Q-learning for offline reinforcement learning. *arXiv preprint arXiv:2006.04779*, 2020.

[36] Hoang Le, Cameron Voloshin, and Yisong Yue. Batch policy learning under constraints. In *International Conference on Machine Learning*, 2019.

[37] Alex X. Lee, Coline Manon Devin, Yuxiang Zhou, Thomas Lampe, Konstantinos Bousmalis, Jost Tobias Springenberg, Arunkumar Byravan, Abbas Abdolmaleki, Nimrod Gileadi, David Khosid, Claudio Fantacci, Jose Enrique Chen, Akhil Raju, Rae Jeong, Michael Neunert, Antoine Laurens, Stefano Saliceti, Federico Casarini, Martin Riedmiller, Raia Hadsell, and Francesco Nori. Beyond pick-and-place: Tackling robotic stacking of diverse shapes. In *Conference on Robot Learning*, 2021.

[38] Sergey Levine, Chelsea Finn, Trevor Darrell, and Pieter Abbeel. End-to-end training of deep visuomotor policies. *Journal of Machine Learning Research*, 2016.

[39] Sergey Levine, Aviral Kumar, George Tucker, and Justin Fu. Offline reinforcement learning: Tutorial, review, and perspectives on open problems. *arXiv preprint arXiv:2005.01643*, 2020.

13

[40] Lihong Li, Wei Chu, John Langford, and Robert E Schapire. A contextual-bandit approach to personalized news article recommendation. In *World Wide Web*, 2010.

[41] Lihong Li, Wei Chu, John Langford, and Xuanhui Wang. Unbiased offline evaluation of contextual-bandit-based news article recommendation algorithms. In *ACM international conference on Web search and data mining*, 2011.

[42] Qiang Liu, Lihong Li, Ziyang Tang, and Dengyong Zhou. Breaking the curse of horizon: Infinite-horizon off-policy estimation. In *Advances in Neural Information Processing Systems*, 2018.

[43] Daniel J Lizotte, Tao Wang, Michael H Bowling, and Dale Schuurmans. Automatic gait optimization with gaussian process regression. In *International Joint Conference on Artificial Intelligence*, 2007.

[44] R. Martinez–Cantin, N. de Freitas, E. Brochu, J. Castellanos, and A. Doucet. A Bayesian exploration-exploitation approach for optimal online sensing and planning with a visually guided mobile robot. *Autonomous Robots*, 2009.

[45] Martino Migliavacca, Alessio Pecorino, Matteo Pirotta, Marcello Restelli, and Andrea Bonarini. Fitted policy search: Direct policy search using a batch reinforcement learning approach. In *Workshop on Evolutionary and Reinforcement Learning for Autonomous Robot Systems*, 2010.

[46] Azalia Mirhoseini, Anna Goldie, Mustafa Yazgan, Joe Jiang, Ebrahim Songhori, Shen Wang, Young-Joon Lee, Eric Johnson, Omkar Pathak, Sungmin Bae, et al. Chip placement with deep reinforcement learning. *arXiv preprint arXiv:2004.10746*, 2020.

[47] Volodymyr Mnih, Koray Kavukcuoglu, David Silver, Alex Graves, Ioannis Antonoglou, Daan Wierstra, and Martin Riedmiller. Playing Atari with deep reinforcement learning. *arXiv preprint arXiv:1312.5602*, 2013.

[48] Remi Munos, Tom Stepleton, Anna Harutyunyan, and Marc Bellemare. Safe and efficient off-policy reinforcement learning. In *Advances in Neural Information Processing Systems*, 2016.

[49] Ofir Nachum, Yinlam Chow, Bo Dai, and Lihong Li. Dualdice: Behavior-agnostic estimation of discounted stationary distribution corrections. In *Advances in Neural Information Processing Systems*, 2019.

[50] Xinkun Nie, Emma Brunskill, and Stefan Wager. Learning when-to-treat policies. *arXiv preprint arXiv:1905.09751*, 2019.

[51] Tom Le Paine, Cosmin Paduraru, Andrea Michi, Caglar Gulcehre, Konrad Zolna, Alexander Novikov, Ziyu Wang, and Nando de Freitas. Hyperparameter selection for offline reinforcement learning. *arXiv preprint arXiv:2007.09055*, 2020.

[52] Jack Parker-Holder, Aldo Pacchiano, Krzysztof M Choromanski, and Stephen J Roberts. Effective diversity in population based reinforcement learning. In *Advances in Neural Information Processing Systems*, 2020.

[53] Doina Precup. Eligibility traces for off-policy policy evaluation. *Computer Science Department Faculty Publication Series*, 2000.

[54] Doina Precup, Richard S. Sutton, and Satinder P. Singh. Eligibility traces for off-policy policy evaluation. In *International Conference on Machine Learning*, 2000.

[55] Carl Edward Rasmussen and Christopher K. I. Williams. *Gaussian Processes for Machine Learning (Adaptive Computation and Machine Learning)*. The MIT Press, 2005.

[56] Julian Schrittwieser, Ioannis Antonoglou, Thomas Hubert, Karen Simonyan, Laurent Sifre, Simon Schmitt, Arthur Guez, Edward Lockhart, Demis Hassabis, Thore Graepel, et al. Mastering Atari, Go, Chess and Shogi by Planning with a Learned Model. *Nature*, 2020.

[57] Bobak Shahriari, Kevin Swersky, Ziyu Wang, Ryan P Adams, and Nando De Freitas. Taking the human out of the loop: A review of Bayesian optimization. *Proceedings of the IEEE*, 2015.

[58] Noah Siegel, Jost Tobias Springenberg, Felix Berkenkamp, Abbas Abdolmaleki, Michael Neunert, Thomas Lampe, Roland Hafner, Nicolas Heess, and Martin Riedmiller. Keep doing what worked: Behavior modelling priors for offline reinforcement learning. In *International Conference for Learning Representations*, 2020.

[59] David Silver, Aja Huang, Chris J Maddison, Arthur Guez, Laurent Sifre, George Van Den Driessche, Julian Schrittwieser, Ioannis Antonoglou, Veda Panneershelvam, Marc Lanctot, et al. Mastering the game of Go with deep neural networks and tree search. *Nature*, 2016.

[60] J. Snoek, H. Larochelle, and R. P. Adams. Practical Bayesian optimization of machine learning algorithms. In *Advances in Neural Information Processing Systems*, 2012.

[61] Niranjan Srinivas, Andreas Krause, Sham Kakade, and Matthias Seeger. Gaussian process optimization in the bandit setting: No regret and experimental design. In *International Conference on Machine Learning*, 2010.

[62] Niranjan Srinivas, Andreas Krause, Sham M Kakade, and Matthias Seeger. Gaussian process optimization in the bandit setting: No regret and experimental design. *arXiv preprint arXiv:0912.3995*, 2009.

[63] Yanan Sui, Alkis Gotovos, Joel Burdick, and Andreas Krause. Safe exploration for optimization with gaussian processes. In *International Conference on Machine Learning*, 2015.

[64] Richard S Sutton, Hamid Reza Maei, Doina Precup, Shalabh Bhatnagar, David Silver, Csaba Szepesvári, and Eric Wiewiora. Fast gradient-descent methods for temporal-difference learning with linear function approximation. In *International Conference on Machine Learning*, 2009.

[65] Richard S Sutton, A Rupam Mahmood, and Martha White. An emphatic approach to the problem of off-policy temporal-difference learning. *Journal of Machine Learning Research*, 2016.

[66] Yuval Tassa, Saran Tunyasuvunakool, Alistair Muldal, Yotam Doron, Siqi Liu, Steven Bohez, Josh Merel, Tom Erez, Timothy Lillicrap, and Nicolas Heess. dm_control: Software and tasks for continuous control. *arXiv preprint arXiv:2006.12983*, 2020.

[67] Georgios Theocharous, Philip S Thomas, and Mohammad Ghavamzadeh. Personalized ad recommendation systems for life-time value optimization with guarantees. In *International Joint Conference on Artificial Intelligence*, 2015.

[68] Masatoshi Uehara, Jiawei Huang, and Nan Jiang. Minimax weight and Q-function learning for off-policy evaluation. In *International Conference on Machine Learning*, 2020.

[69] Hado Van Hasselt, Arthur Guez, and David Silver. Deep reinforcement learning with double Q-learning. In *National Conference on Artificial Intelligence (AAAI)*, 2016.

[70] Cameron Voloshin, Hoang M Le, Nan Jiang, and Yisong Yue. Empirical study of off-policy policy evaluation for reinforcement learning. *arXiv preprint arXiv:1911.06854*, 2019.

[71] Ziyu Wang, Alexander Novikov, Konrad Żołna, Jost Tobias Springenberg, Scott Reed, Bobak Shahriari, Noah Siegel, Josh Merel, Caglar Gulcehre, Nicolas Heess, and Nando de Freitas. Critic regularized regression. In *Advances in Neural Information Processing Systems*, 2020.

[72] Mengjiao Yang, Bo Dai, Ofir Nachum, George Tucker, and Dale Schuurmans. Offline policy selection under uncertainty. *arXiv preprint arXiv:2012.06919*, 2020.

[73] Mengjiao Yang, Ofir Nachum, Bo Dai, Lihong Li, and Dale Schuurmans. Off-policy evaluation via the regularized lagrangian. *arXiv preprint arXiv:2007.03438*, 2020.

[74] Tianhe Yu, Garrett Thomas, Lantao Yu, Stefano Ermon, James Zou, Sergey Levine, Chelsea Finn, and Tengyu Ma. MOPO: Model-based offline policy optimization. *arXiv preprint arXiv:2005.13239*, 2020.

[75] Michael R Zhang, Tom Le Paine, Ofir Nachum, Cosmin Paduraru, George Tucker, Ziyu Wang, and Mohammad Norouzi. Autoregressive dynamics models for offline policy evaluation and optimization. *arXiv preprint arXiv:2104.13877*, 2021.

A Algorithmic details

A.1 GP model

Following the data generative process in Sec. 2.2, the hierarchical probabilistic model of all the latent policy values μ, OPE estimates ρ, and episodic returns r[5] at the given K policies $\{\pi_k\}_{k=1}^K$ is given as follows:

$$
\begin{aligned}
\mu_1, \ldots, \mu_K &\sim \mathcal{N}(m\mathbf{1}_K, \mathbf{K}) \\
\rho_k &\overset{i.i.d.}{\sim} \mathcal{N}(\mu_k, \sigma_\rho^2), \forall k \in \{1, \ldots, K\} \\
r_k^i &\overset{i.i.d.}{\sim} \mathcal{N}(\mu_k, \sigma_r^2), \forall i \in \{1, \ldots, N_k\} \\
\sigma_\rho^2 &\sim \mathrm{IG}(\alpha, \beta) \\
\sigma_r^2 &\sim \mathrm{IG}(\alpha, \beta) \,,
\end{aligned}
\tag{9}
$$

where the mean m is a constant hyper-parameter and the covariance $\mathbf{K}(\pi_k, \pi_k') = \mathcal{K}(\pi_k, \pi_{k'})$. The kernel function is defined as

$$
\begin{aligned}
\mathcal{K}(\pi_k, \pi_{k'}) &= \sigma_k^2 \exp(-\bar{d}(\pi_k, \pi_{k'})/l) \\
\bar{d}(\pi_k, \pi_{k'}) &= \mathbb{E}_{s \sim \mathcal{D}'} \, d(\pi_k(s), \pi_{k'}(s)) \\
\sigma_k^2 &\sim \mathrm{IG}(\alpha, \beta) \,,
\end{aligned}
\tag{10}
$$

with $\mathcal{D}'$ being a fixed set of states that is randomly subsampled from the entire offline dataset $\mathcal{D}$. σ_k^2 and l are hyper-parameters. We assume an uninformative prior for l.

The posterior distribution of $[\mu_1, \ldots, \mu_K]$ given all the observation and hyper-parameters is also a multivariate normal distribution given in Eq. 5. The log-marginal likelihood of all the hyper-parameters with μ_k's integrated out is as follows,

$$
\begin{aligned}
&\log P(\boldsymbol{\rho}, \{\mathbf{r}_k\}_k, \sigma_\rho^2, \sigma_r^2, \sigma_k^2 | m, l) \\
&= -\frac{1}{2} \log |\boldsymbol{\Sigma}| - \frac{1}{2} \mathbf{y}^T \boldsymbol{\Sigma} \mathbf{y} - \frac{1}{2} \left(K \log(\sigma_\rho^2) + n \log(\sigma_r^2) - \sum_{k=1}^K \log(\boldsymbol{\Lambda}_{kk}) \right) \\
&\quad - \frac{1}{2} \sum_{k=1}^K \left(\frac{\rho_k^2}{\sigma_\rho^2} + \frac{1}{\sigma_r^2} \sum_{i=1}^{N_k} (r_k^i)^2 - \frac{\mathbf{y}_k^2}{\boldsymbol{\Lambda}_{kk}} \right) + \log \mathrm{IG}(\sigma_\rho^2) + \log \mathrm{IG}(\sigma_r^2) + \log \mathrm{IG}(\sigma_k^2) + \text{const.} \,,
\end{aligned}
\tag{11}
$$

where $n = \sum_k N_k$ and const. is a constant.

A.2 Independent policy value baseline model (IND)

In Sec. 4.2, we consider a baseline model with independent policy value distributions as follows,

$$
\begin{aligned}
r_k^i &\overset{i.i.d.}{\sim} \mathcal{N}(\mu_k, \sigma_{k,r}^2), \forall i, \text{ with} \\
\mu_k &\overset{i.i.d.}{\sim} \mathcal{N}(\rho_k, \sigma_{k,\rho}^2), \forall k \\
\sigma_{k,\rho}^2 &\overset{i.i.d.}{\sim} \mathrm{IG}(\alpha, \beta), \forall k \\
\sigma_{k,r}^2 &\overset{i.i.d.}{\sim} \mathrm{IG}(\alpha, \beta), \forall k.
\end{aligned}
\tag{12}
$$

---

[5]We assume Gaussian distribution for the noise model, but if the form of return noise distribution is known in advance, it can replace the Gaussian noise model and approximate GP inference can be performed.

Since the model is i.i.d. across policies, we omit the index k for ease of notation. The posterior distribution of μ given $\mathbf{r} = [r^1, \ldots, r^N]$, σ_r^2 and σ_ρ^2 is then given as

$$\mu \sim \mathcal{N}(m, s^2)$$

$$m = \frac{\sum_{i=1}^N r^i + (\sigma_r^2/\sigma_\rho^2)\rho}{N + (\sigma_r^2/\sigma_\rho^2)}$$

$$s^2 = \frac{\sigma_r^2}{N + (\sigma_r^2/\sigma_\rho^2)} \,. \tag{13}$$

The log-marginal likelihood with μ integrated out can be derived as

$$\log P(\rho, \mathbf{r}, \sigma_\rho^2, \sigma_r^2|)$$

$$= -\frac{1}{2}\left(\log(\sigma_\rho^2) + N\log(\sigma_r^2) - \log(s^2)\right) - \frac{1}{2}\left(\frac{\rho^2}{\sigma_\rho^2} + \frac{1}{\sigma_r^2}\sum_{i=1}^N (r^i)^2 - \frac{y^2}{s^2}\right)$$

$$+ \log \mathrm{IG}(\sigma_\rho^2) + \log \mathrm{IG}(\sigma_r^2) + \text{const.} \,, \tag{14}$$

where const. is a constant.

A.3 Hyperparameter fitting

We fit the hyperparameters in both models whenever a new observation is obtained by searching for the maximum a posteriori (MAP) estimate using a few steps of gradient descent on the log-marginal likelihood.

Fitting the hyper-parameters at the beginning with few observations is challenging. When we do not use OPE to warm start GP inference such as in GP+UCB and GP+UNIFORM, we start by randomly selecting the first 5 policies to execute. Besides, it is important in this case to apply a prior for hyperparameters to prevent variance from shrinking towards zero. When OPE is available, we find neither of these techniques is required for a robust estimation and we can start fitting the hyperparameters of GP from the first step.

A.4 Hyperparameter values

The initial values of the hyperparameters of GP and our method in general are listed next. We set the GP hyperparameters based on the statistics about the policy returns from the offline dataset. The same hyperparameters are used for all the domains. The discounted returns in Atari domain are very different in scale from the other domains. To ensure that the same hyperparameters are applicable to all domains, we rescale returns in Atari to the same range of means and variances as other domains based on the statistics from the datasets for offline RL.

- We find using a constant value $\sqrt{\beta_i} = 5$ in GP-UCB works well across different budgets, Bayesian models, and environments, although a more sophisticated scheduling [62, 4, 26] could further improve the results.
- The hyperparameters of the prior for IND were set to: $\alpha = 1, \beta = 1000$.
- Observation noise variance of GP was set to the initial value of 1000 or prior with $\alpha = 1, \beta = 200$ when the prior is used. Initial value of the offset m was 0.
- For GP optimisation we used Adam optimiser with learning rate 0.001 and 1000 optimisation steps per observation update. $\beta_1 = 0.9, \beta_2 = 0.999$.
- To compensate to the non-zero mean in the GP, we use a constant component in the kernel with trainable variance parameter initially set to 10. When the prior is used, we set $\alpha = 1, \beta = 200$ in all the experiments.

A.5 Kernel selection

In our preliminary experiments, we experimented with a few ways to compute the kernel over policies. To quickly select promising ideas, we tested them in a simple regression task where we split all

policies with their true returns into training and testing sets and predict the returns of the test policies based on the training policies. Then, we select the kernel that gives the highest log likelihood and lowest squared prediction error. We choose the best type of kernel using 3 dm-control environments (`cartpole_swingup`, `fish_swim` and `manipulator_insert_ball`) and apply the same kernel to all tasks of both domains in the experiments. The most important variations of the kernel that we studied are enumerated below. We highlight the variant that was used in the final experiments.

- As a subset $\mathcal{D}'$ of states for computing policy's actions, we select 1000 states. We tried to use 1) *random states*, 2) initial states, 3) states with high rewards, 4) states with low rewards, 5) states in the trajectories with high returns, 6) states in the trajectories with low returns. Several options looked promising, including 1, 2, 4. At the end we chose the simplest option that yielded good results (1).

- As a way to construct a kernel from the policy actions on several states, we considered: 1) *multiplication of kernels on separate states*, 2) concatenating action predictions into a single feature vector. We chose kernel multiplication because we found in our experiments that concatenating the action in a single vector makes the distances not very informative. This happens because the dimensionality of the policy representation becomes very high.

- After obtaining the distances matrix for the policies, we compute the kernel. We tried 1) RBF, 2) Matérn $5/2$, 3) Matérn $3/2$, 4) *Matérn $1/2$* kernels. While the difference between these versions was not large, the less smooth kernel Matérn $1/2$ performed slightly better and reflected our intuition that the return of policies trained with different algorithms can change quickly (Fig. 3, right).

A.6 Bayesian optimization algorithm

The pseudo-code of the Bayesian optimization algorithm for both models is presented in algorithm 1.

Algorithm 1: UCB algorithm for active offline policy selection

---

Data: Environment env, set of policies $\{\pi_k\}$, $1 \leq k \leq K$, number of initial random samples n_{init}, total number of steps n, (optional) OPE estimates $\{\rho_k\}$
Result: Final recommendation $\hat{k}$
for $i : 1 \rightarrow n$ **do**
    if $i \leq n_{\text{init}}$ **then**
        Sample a policy k_i uniformly from $\{1, 2, \ldots, K\}$
    else
        Fit hyper-parameters by maximizing the log-marginal likelihood (Eq. 11 or Eq. 14) with all the return samples r_i and OPE estimates ρ_k;
        Update the posterior of $\boldsymbol{\mu}$ using Eq. 5 or Eq. 13;
        Compute the UCB acquisition function $u_i(k)$ for every policy k using Eq. 7;
        Choose a policy $k_i = \arg\max_k u_i(k)$;
    end
    Apply policy π_{k_i} in env for one episode and receive the discounted episodic return r_i;
end
Maximize the log-marginal likelihood (Eq. 11 or Eq. 14) wrt the hyper-parameters using Adam;
Update the posterior of $\boldsymbol{\mu}$ using Eq. 5 or Eq. 13;
return $\hat{k} = \arg\max_k \mathbf{m}_k$ *with* $\mathbf{m}_k$ *being the posterior mean of k-th policy*

B   Domains details

In this section, we present the statistics about our domains of interest: dm-control, MPG and Atari. We describe how we obtain the policies and present the statistics about the returns.

B.1   Dm-control

In dm-control domain we use policies from the DOPE benchmark [20], which results in a diverse set of policies with varying algorithms (D4PG, ABM, CRR), hyperparameters like learn-
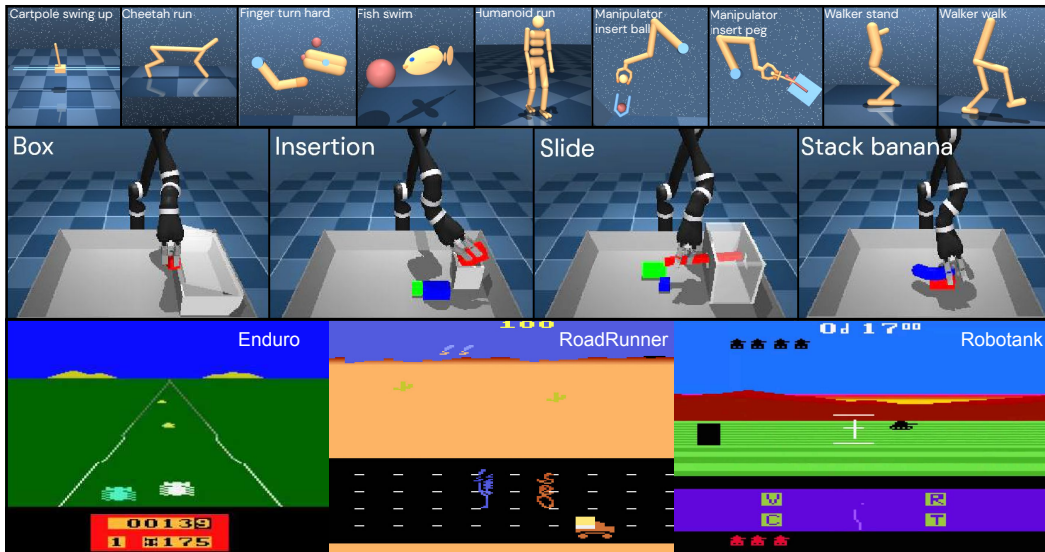
Figure 10: Environments used in the experiments. Top: 9 environments from the dm-control domain. Middle: 4 environments from the MPG domain. Bottom: 3 game environments from Atari domain.

task	stdev	min return	max return
cartpole_swingup	6.488	0.451	31.504
cheetah_run	5.504	6.933	36.291
finger_turn_hard	14.055	8.613	60.971
fish_swim	3.208	8.097	18.755
humanoid_run	8.993	0.566	30.117
manipulator_insert_ball	2.825	3.668	13.801
manipulator_insert_peg	2.306	4.668	11.249
walker_stand	13.173	39.180	85.533
walker_walk	13.973	11.950	74.719

Table 3: Statistics about the policies in dm-control: the return of the worst policy, of the best policy and standard deviation of the policies returns.

ing rate, and number of training steps, giving up to 96 policies per task, and a diverse range of returns. There are 9 environments as shown in the top row of Fig. 10: cartpole_swingup, cheetah_run, finger_turn_hard, fish_swim, humanoid_run, manipulator_insert_ball, manipulator_insert_peg, walker_stand, walker_walk. There is a significant gap between the scores of the badly-performing and well-performing policies. Tab. 3 shows the standard deviation, minimum and maximum returns of the policies from the dataset.

The success of the active policy selection strategy in each experiment depends on the relation between the variance of the returns of the policies in the dataset and the variance of the returns that a single policy renders. To understand this relationship better in Fig. 11 we show for each environment: 1) the distribution of policy OPE metrics as a function of true scores at the top, and 2) the histogram of the episodic returns for a single randomly selected policy (highlighted and connected by a dashed line) at the bottom. We observe that in some cases (for example, in finger_turn_hard, fish_swim, walker_walk) the variance of episodic returns is greater than the variance of the policies true scores. This is particularly challenging for any policy selection that involves the online component. Furthermore, we also observe that in some cases OPE scores are not well correlated with the true scores (for example, fish_swim, humanoid_run, manipulator_insert_ball, manipulator_insert_peg). In this case, on one hand, relying on OPE scores makes policy selection more challenging, but on the other hand, it leaves the biggest potential for improvement by involving the online evaluation.
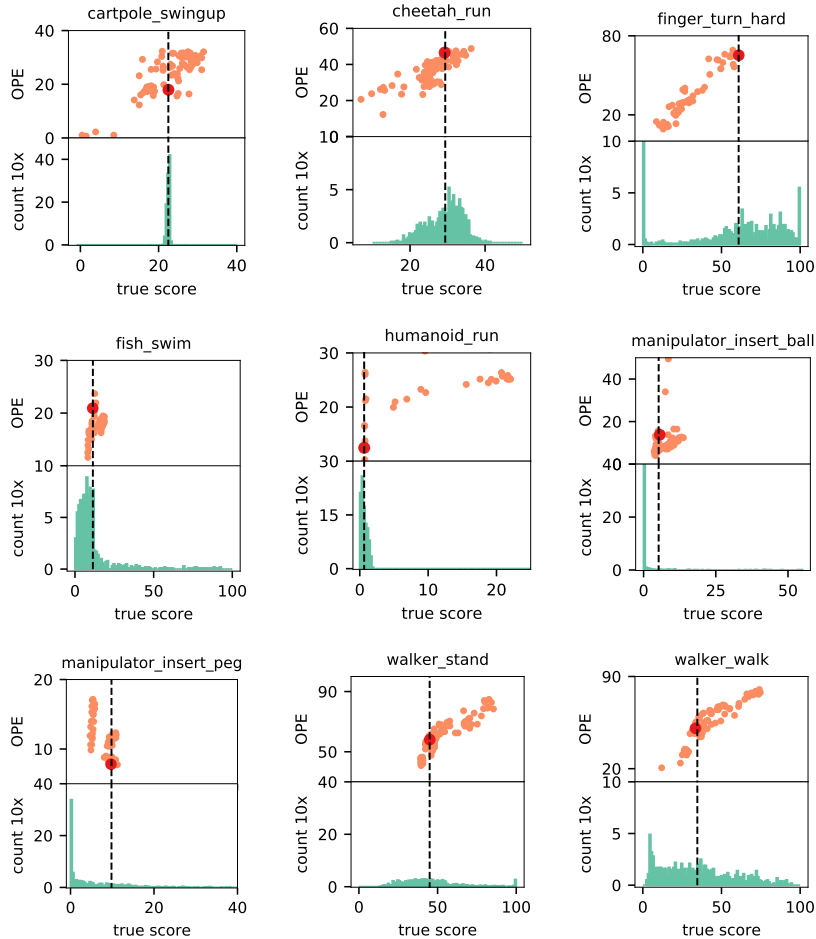
Figure 11: For each environment in dm-control we show 1) the distribution of policy OPE metrics as a function of true scores at the top (in orange), and 2) the histogram of the episodic returns for a single randomly selected policy (in green) at the bottom. The randomly selected policy is highlighted with a red dot on the top and it is connected by a dashed line to the mean values in the histogram.

B.2 MPG

To generate policies for the environments in MPG domain we follow the protocol in [51]. For each task, we generate up to 256 policies trained with various algorithms (BC, D4PG, and CRR), and hyperparameters including number of hidden units $(64, 1024)$, number of blocks $(1, 5)$, learning rate $(1 \times 10^{-3}, 1 \times 10^{-5})$, learning steps (50k, 250k, 25k), and for CRR the beta parameter $(0.1, 10)$. This ensures there is a diverse range of policies that span the range of possible returns. There are four tasks in MPG domain: `box`, `insertion`, `slide`, and `stack_banana` as shown in the middle row of Fig. 10. We include MPG as a challenging domain where policies are learnt from high dimensional images and training online policy takes thousands of trajectories (around 8000) even when human demonstrations are included.

The policies in this domain also exhibit a significant gap and large variance in the scores of the badly-performing and well-performing policies as it is demonstrated by the statistics in Tab. 4. As this is a challenging domain, in all the environments, the worst policy achieves 0 (lowest possible) regret.

In Fig. 12 we study again the relationship between the distribution of policy OPE metrics and true scores, as well as the distribution of the episodic returns for a random policy. In all environments, the variance of episodic returns is comparable or even greater than the variance of the policies true scores. In some cases, like in `box` and `stack_banana` the OPE scores are almost perfectly correlated with

task	stdev	min return	max return
box	19.711	0.0	64.58
insertion	15.808	0.0	52.42
slide	14.622	0.0	52.17
stack_banana	18.420	0.0	58.74

Table 4: Statistics about the policies in MPG: the return of the worst policy, of the best policy and standard deviation of the policies returns.
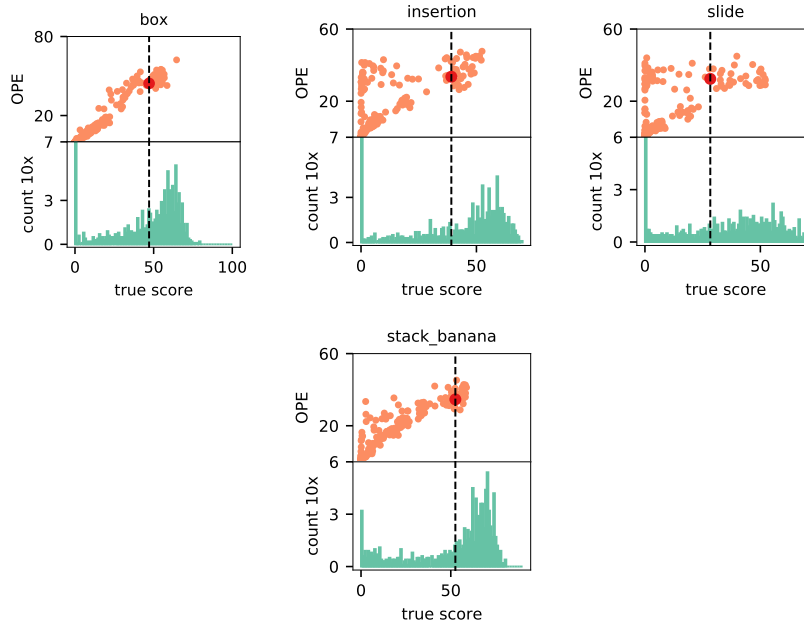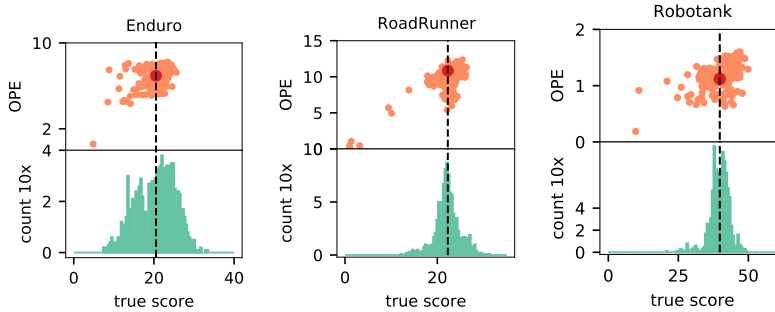

Figure 12: For each environment in MPG we show 1) the distribution of policy OPE metrics as a function of true scores at the top (in orange), and 2) the histogram of the episodic returns for a single randomly selected policy (in green) at the bottom. The randomly selected policy is highlighted with a red dot on the top and it is connected by a dashed line to the mean values in the histogram.

the true returns, which makes the OPE baseline very hard to beat. Even when OPE scores are not perfectly correlated with the true returns, like in the `insertion` environment, it may still be very informative for the task of selecting the *best* policy. There is the biggest potential for improvement over OPE in `slide` environment. Also, notice that many policies have a peak value in the histogram at value 0 (including policies with high average return). This property makes the sparse online evaluation particularly challenging.

B.3 Atari

We choose Atari in order to test our method on an established discrete control offline RL domain where training an online policy from pixels is challenging and requires thousands of trajectories. We follow the protocol in [23] to train 210 policies with different architectures and hyperparameter for each of three Atari games: `Enduro`, `RoadRunner`, and `Robotank` as shown in Fig. 10, bottom row. `Enduro` is previously used as an OPE benchmark [70]. We include `RoadRunner` and `Robotank` to cover a range of difficulty and reward scales presented in the Atari benchmark. The policies cover a diverse range of methods and this results in the most diverse set of policies for the experiments in this paper: DDQN [69], BCQ [21], REM [2], IQN [13], CQL [35], and BVE [22]. We use grid search over the following hyperparameters: learning rate for all algorithm (3×10^{-5}, 1×10^{-4}, 3×10^{-4}), the pessimism regularizer in CQL (1×10^{-3}, 1×10^{-2}, 1×10^{-1}, 1, 2), the threshold parameter in BCQ (0.1, 0.25, 0.5, 0.75). Each algorithm with a hyperparameter setting is trained on 5 datasets generated by DQN snapshots trained with five different seeds as described in [2].

task	stdev	min return	max return
Enduro	3.198	4.848	25.617
Robotank	5.509	9.786	49.898
RoadRunner	3.867	1.012	26.298

Table 5: Statistics about the policies in Atari: the return of the worst policy, of the best policy and standard deviation of the policies returns.

Figure 13: For each environment in Atari we show 1) the distribution of policy OPE metrics as a function of true scores at the top (in orange), and 2) the histogram of the episodic returns for a single randomly selected policy (in green) at the bottom. The randomly selected policy is highlighted with a red dot on the top and it is connected by a dashed line to the mean values in the histogram.

As in other domains, there is a significant gap between the scores of the badly-performing and well-performing policies as indicated in the Tab. 5. In Fig. 13 we show the relationship between the distribution of policy OPE metrics and true scores, as well as the distribution of the episodic returns for one of the policies. The OPE scores are correlated, but the correlation is far from perfect and there is space for improvement by including the online trajectories.

C   Results by task

While subsection 4.3 and subsection 4.4 present the aggregated results across all tasks where each task is normalised by the gap between policies, in this section we present figures for each task separately. We discuss the variability of the results across different environments and explain the reasons for this variability.

C.1   Dm-control

Similar to Fig. 5, Fig. 14 shows the comparison between our proposed method A-OPS, completely offline policy selection with OPE and completely online selection with IND+UNIFORM on each of 9 task from dm-control. Depending on the quality of the initial OPE values and the variance of the policy returns (see Fig. 11), A-OPS may take different number of trajectories before it outperforms all the baselines, but usually it only takes a few steps. Eventually, A-OPS reaches the best performance with the limited budget.

Similar to Fig. 6 (first row), Fig. 15 shows the contribution of each of the components of the method. Our method A-OPS is preferable in all environments across a wide range of interaction budget except for cheetah_run with less than 50 trajectories. Again we observe that modelling correlated policies as in GP performs better than modelling independent policies as in IND, active policy selection as in UCB is better than uniform policy selection as in UNIFORM. In manipulator tasks, no method achieves a regret as low as in other tasks. We believe that the main reasons for this are 1) low performance of the initial OPE estimates and 2) the skewed distribution of episodic returns of all policies where most returns are close to 0 (see Fig. 11).

Similar to Fig. 6 (second row), Fig. 16 shows the contribution of each of the components of the method in case when OPE is not used. It is clear that the results are significantly worse than when
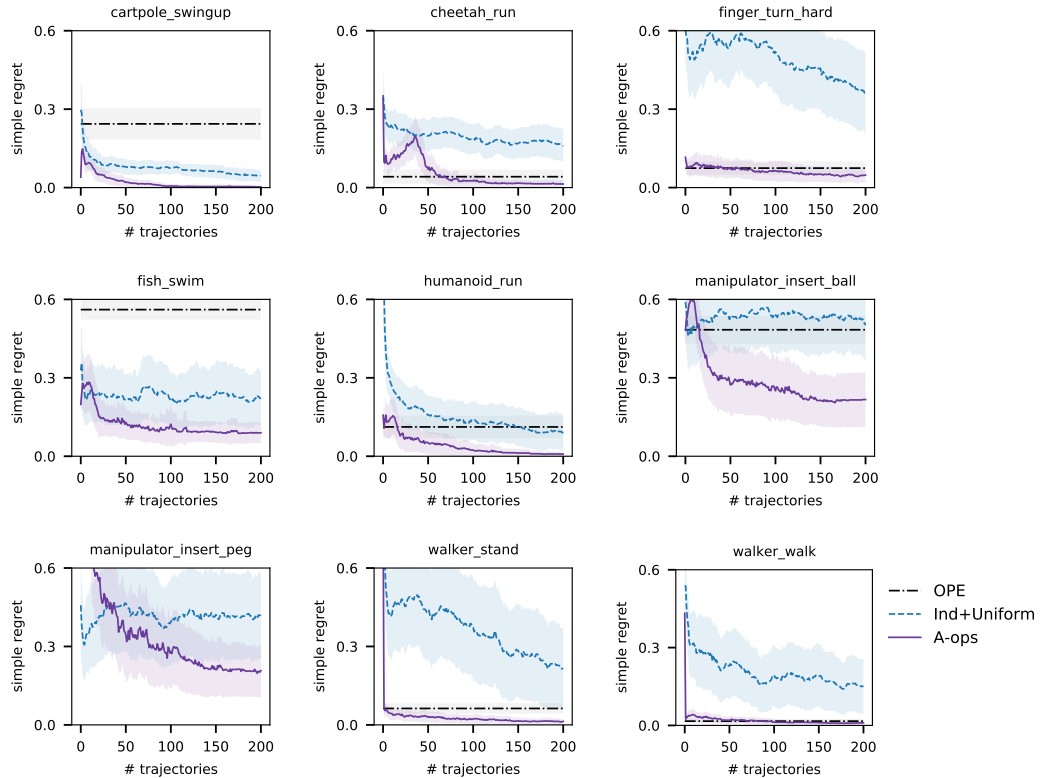
Figure 14: Comparison of A-OPS approach, offline policy selection with OPE, and online policy selection with IND+UNIFORM on each environment in dm-control domain. The results are averaged across 100 experiments. We do not show OPE performance in `manipulator_insert_peg` in order to respect the y-axis limits. The value is 0.88 as D4PG policies are highly overestimated. Shaded areas show standard deviation of the mean. Our method A-OPS quickly surpasses the baselines and achieves the lowest regrets.

using OPE (Fig. 15) which clearly indicated the benefit of OPE component in A-OPS. When OPE estimates are not available, the combination of modelling correlated policies as in GP and intelligent policy selection as in UCB gives the best results on average. It performs better than the next best method in 6 environments, slightly worse in 1 and approximately the same in 2. On average, the GP+UCB strategy is the best when OPE estimates are not available.

C.2 MPG

Similar to Fig. 5, Fig. 17 shows the comparison between our proposed method A-OPS, completely offline policy selection with OPE and completely online selection with IND+UNIFORM on each of 4 tasks from MPG. OPE performs exceedingly well in 3 of 4 tasks, getting regret close to zero for 2 tasks (see Fig. 12 with plot of OPE vs the ground truth). Nevertheless we manage to perform about as well or better on all of the tasks: In 2 environments, A-OPS only approaches the OPE baseline, but in the other 2 environments, A-OPS quickly surpasses OPE. It makes the most improvement in the `slide` task. This difference in the performance in different tasks is due to the variability of performance of OPE method and the variance in returns in the online policy executions. High return variance requires a large number of environment interactions for an online policy evaluation method to provide accurate estimates. However, the most important observation is that A-OPS achieves a small regret in all environments.

Similar to Fig. 6 (first row), Fig. 18 shows the contribution of each of the components of the method when using OPE. Our method A-OPS is preferable in all environments across a wide range of interaction budgets. The same observation as before holds: modelling correlated policies as in GP performs better than modelling independent policies as in IND, active policy selection as in UCB is better than uniform policy selection as in UNIFORM.
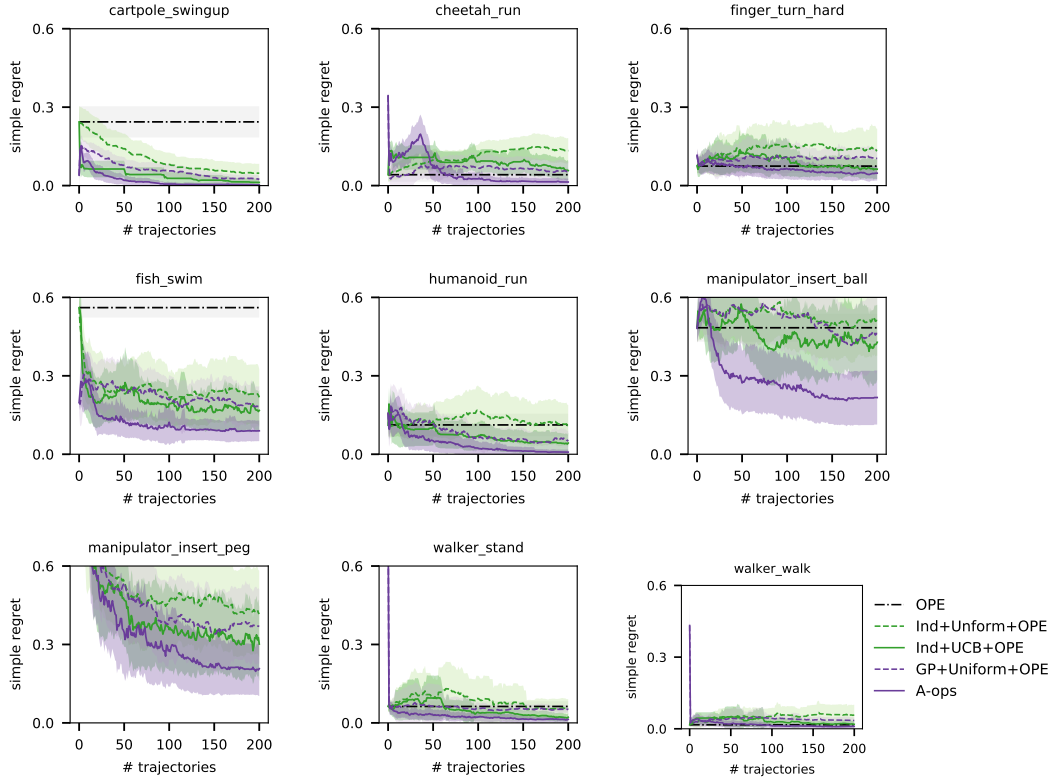
Figure 15: Ablations. In 9 environments of dm-control domain, we ablate two components of our approach when using OPE metrics. 1) The choice of policy model: GP (purple) and independent (green). 2) The policy selection strategy: active (dark, solid line) and uniform sampling (bright, dashed line). We do not show OPE performance in `manipulator_insert_peg` in order to respect the y-axis limits. The value is 0.88 as D4PG policies are highly overestimated. In general, active is better than uniform, methods that exploit policy correlation are better than methods that do not.

Similar to Fig. 6 (second row), Fig. 19 shows the contribution of each of the components of the method in case when OPE is not used. As before, the results are significantly worse than when using OPE (Fig. 18). When OPE estimates are not available, the combination of modelling correlated policies as in GP and intelligent policy selection as in UCB gives the best results in each task. Notice the degraded performance of IND+UCB in the first 200 iterations (mostly exploration stage). This happens because each policy is treated independently and until each of them is executed (200 policies) the regret is quite high. Modelling correlation between the policies as in GP methods helps to alleviate this problem.

C.3 Atari

Similar to Fig. 5, Fig. 20 shows the comparison between our proposed method A-OPS, completely offline policy selection with OPE and completely online selection with IND+UNIFORM on each of 3 Atari games that we consider. Due to the variance of the returns of the policies in this domain, it takes a large number of environment interactions for an online policy evaluation method to provide accurate estimates and in all environments offline evaluation is better. However, A-OPS method outperforms other baselines with only a small amount of environment interactions.

Similar to Fig. 6 (first row), Fig. 21 shows the contribution of each of the components of the method. Our method A-OPS is preferable in all environments across a wide range of interaction budgets. The same observation as before holds: modelling correlated policies as in GP performs better than modelling independent policies as in IND, active policy selection as in UCB is better than uniform policy selection as in UNIFORM. Notice that the gain of A-OPS is particularly pronounced in this
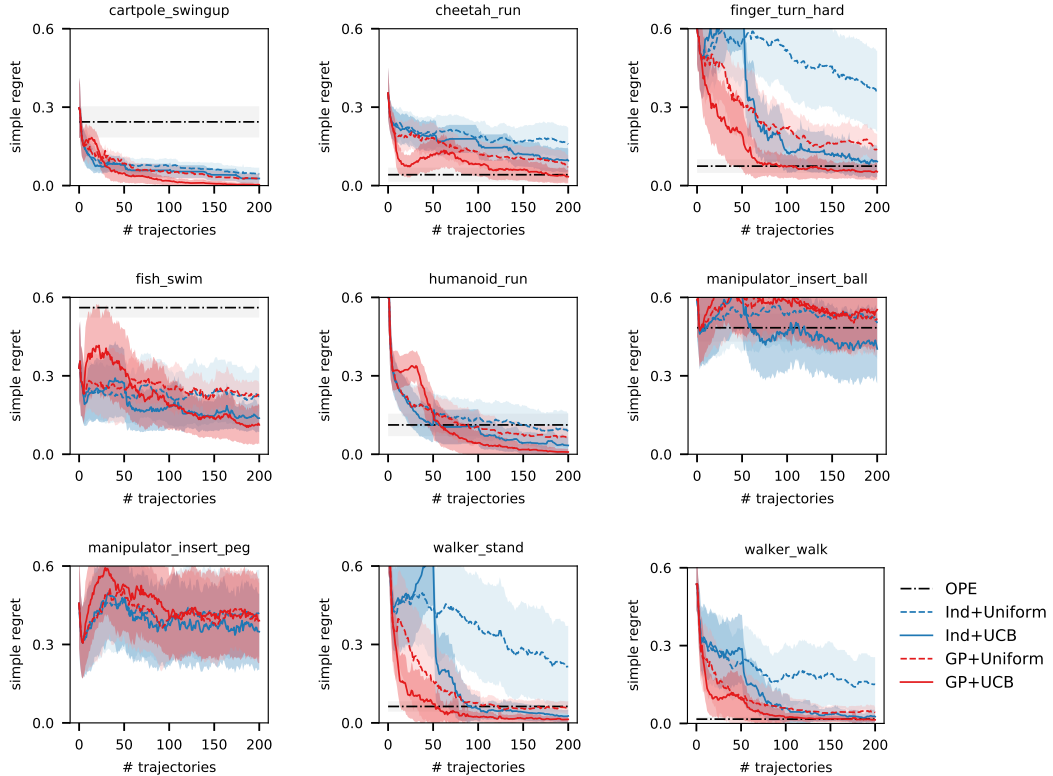
24

Figure 16: Ablations. In 9 environments of dm-control domain, we ablate two components of our approach when NOT using OPE metrics. 1) The choice of policy model: GP (red) and independent (blue). 2) The policy selection strategy: active (dark, solid line) and uniform sampling (bright, dashed line). We do not show OPE performance in `manipulator_insert_peg` in order to respect the y-axis limits. The value is 0.88 as D4PG policies are highly overestimated. In general, active is better than uniform, methods that exploit policy correlation are better than methods that do not.

domain. We attribute it to the data efficiency of our method which is particularly important given a large diversely performing set of policies.

Similar to Fig. 6 (second row), Fig. 22 shows the contribution of each of the components of the method in case when OPE is not used. As before, the results are noticeably worse than when using OPE (Fig. 21). When OPE estimates are not available, the combination of modelling correlated policies as in GP and intelligent policy selection as in UCB gives the best results in each game. Notice the degraded performance of IND+UCB in the first 200 iterations (mostly exploration stage). This happens because each policy is treated independently and until each of them is executed (200 policies) the regret is quite high. Modelling correlation between the policies as in GP methods helps to alleviate this problem and GP+UCB method outperforms all competitors within a small number of trajectories, including OPE method that relies on the offline dataset.

C.4 Discussion of the results by task

The performance of the methods varies from task to task. We highlight that A-OPS does as well as or better than both offline policy selection (OPE) and online policy selection on 9 of 9 dm-control suite tasks, in 2 of 4 MPG tasks and in 3 out of 3 Atari games. The simple regret of A-OPS approaches 0 or is very low in 7 out of 9 dm-control tasks, in 4 out of 4 MPG tasks and in 3 out of 3 Atari tasks. Thus, in cases when A-OPS regret is not very low, it is still much better than that of the alternative methods, and when A-OPS does not outperform some of the methods, its regret remains very low. As a result, despite variability in different tasks, A-OPS is a very reliable method for policy selection. Another reason for variability across different tasks is the fact that we do not address the question of when to stop active policy selection. In some cases, the OPE estimate is so good that there is
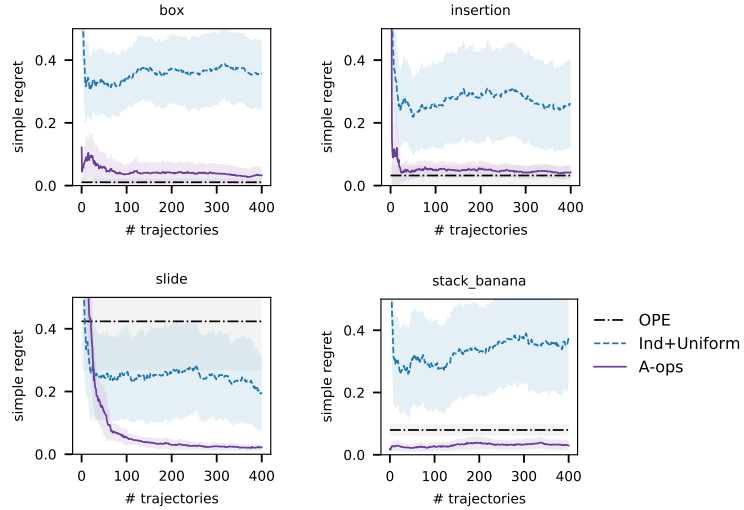
Figure 17: Comparison of A-OPS approach, offline policy selection with OPE, and online policy selection with IND+UNIFORM on each environment in MPG domain. The results are averaged across 100 experiments. Shaded areas show standard deviation of the mean. Our method A-OPS quickly surpasses IND+UNIFORM baseline. A-OPS achieves the regret close to 0 in all environments.
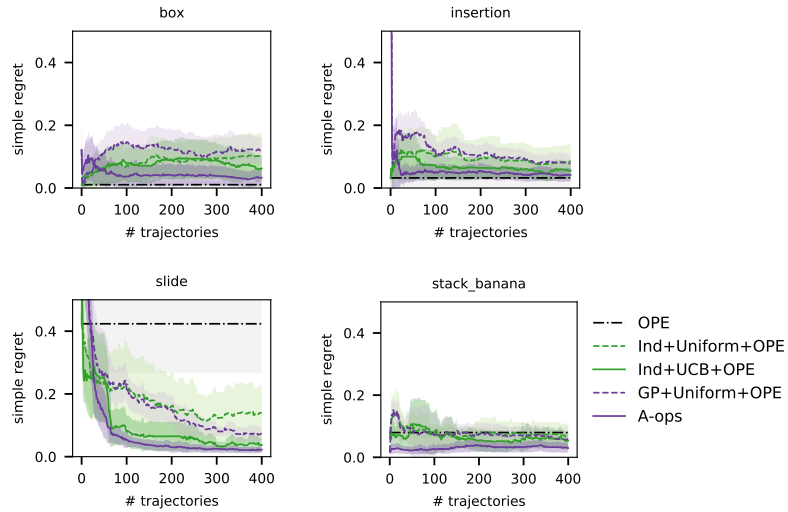

Figure 18: Ablations. In 4 environments of MPG domain, we ablate two components of our approach when using OPE metrics. 1) The choice of policy model: GP (purple) and independent (green). 2) The policy selection strategy: active (dark, solid line) and uniform sampling (bright, dashed line). In general, active is better than uniform, methods that exploit policy correlation are better than methods that do not.

no need for extra online data (for example, as in some of the MPG environments) and in some cases due to the variance of the returns and low correlation of OPE scores with policy returns, even more extensive data collection could be needed. Future work can address this question and derive some recommendations on when to stop policy querying based on statistics in collected data: policy variance, OPE correctness, gap between the policies etc.

In general, the main factors that affect the viability in the A-OPS performance are 1) the distribution of OPE estimates vs ground truth, 2) the variance of returns of a single policy, 3) variance in the returns across available policies. As this information is not available prior to conducting the experiments, it is important that our method A-OPS performs reliably even in the challenging conditions.
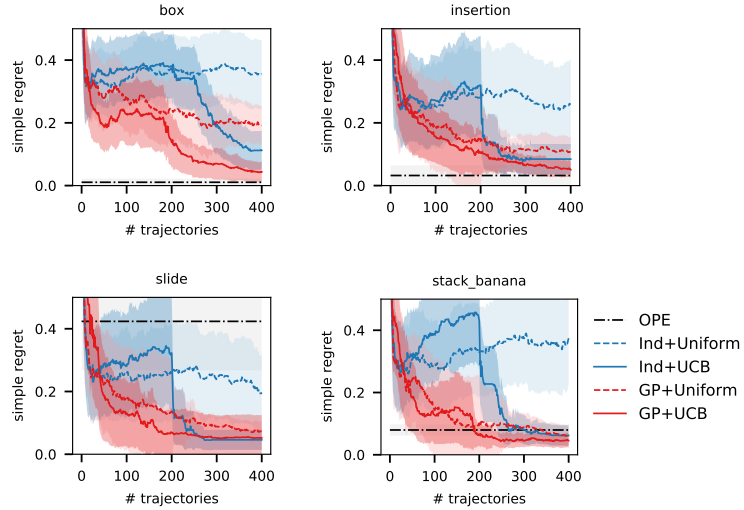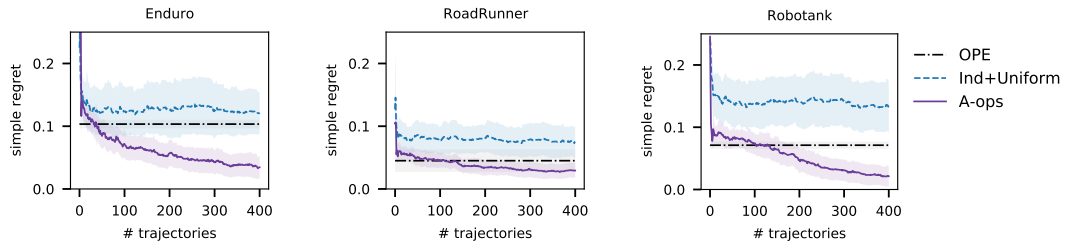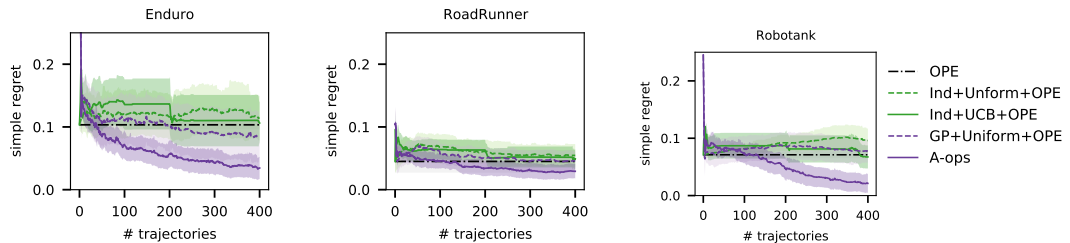
26

Figure 19: Ablations. In 4 environments of MPG domain, we ablate two components of our approach when NOT using OPE metrics. 1) The choice of policy model: GP (red) and independent (blue). 2) The policy selection strategy: active (dark, solid line) and uniform sampling (bright, dashed line). In general, active is better than uniform, methods that exploit policy correlation are better than methods that do not.

Figure 20: Comparison of A-OPS approach, offline policy selection with OPE, and online policy selection with IND+UNIFORM on each environment in Atari domain. The results are averaged across 100 experiments. Shaded areas show standard deviation of the mean. Our method A-OPS quickly surpasses IND+UNIFORM baseline. A-OPS achieves the regret close to 0 in all environments.

Figure 21: Ablations. In 3 environments of MPG domain, we ablate two components of our approach when using OPE metrics. 1) The choice of policy model: GP (purple) and independent (green). 2) The policy selection strategy: active (dark, solid line) and uniform sampling (bright, dashed line). In general, active is better than uniform, methods that exploit policy correlation are better than methods that do not.

Note that the efficiency of A-OPS does not depend on the difficulty of training a policy. For example, training policies from visual input such as in MPG and Atari domains as well as some challenging tasks in dm-control including `humanoid_run`, `manipulator_insert_ball`, `manipulator_insert_peg` require thousands of trajectories to be solved online, but it takes only around 100 of trajectories to identify a good policy.
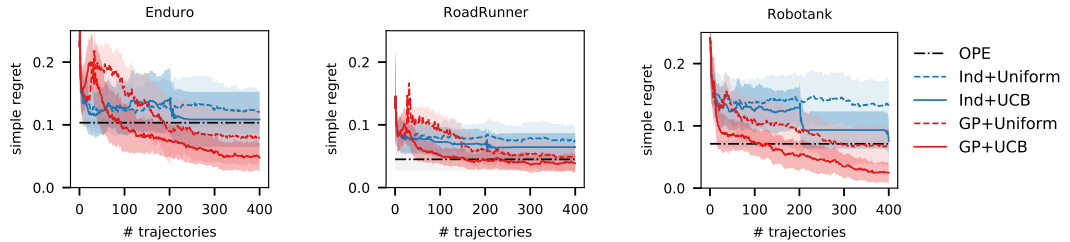
27

Figure 22: Ablations. In 3 environments of Atari domain, we ablate two components of our approach when NOT using OPE metrics. 1) The choice of policy model: GP (red) and independent (blue). 2) The policy selection strategy: active (dark, solid line) and uniform sampling (bright, dashed line). In general, active is better than uniform, methods that exploit policy correlation are better than methods that do not.
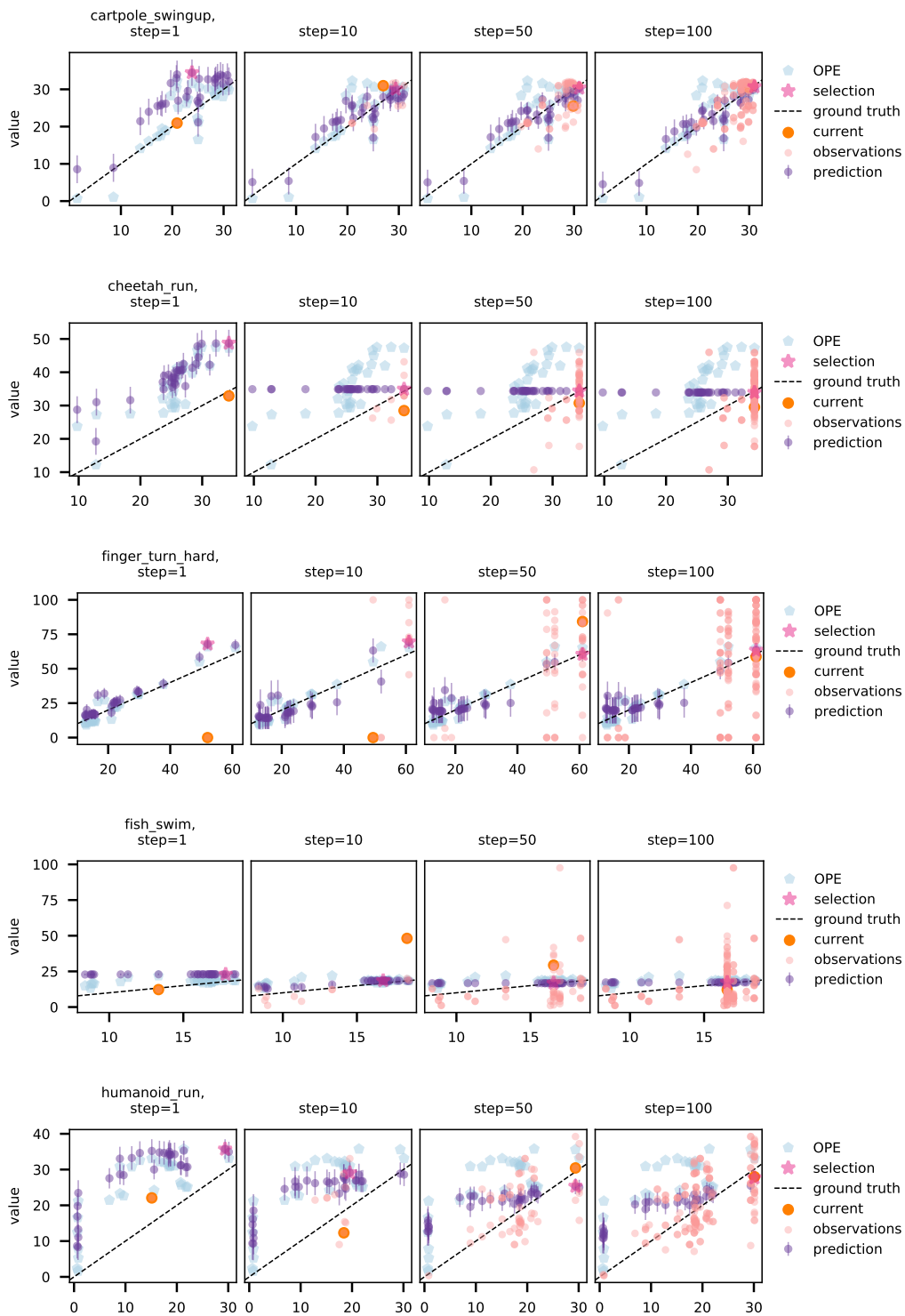
D   Qualitative results by task

We illustrate the behaviour of A-OPS by showing its estimates and selection in one experiment in each environment in Fig. 22 in the same way as in Fig. 9. Each experiment is produced with a fixed random seed and the examples are not curated. Thus, they include both the examples of success in identification of the best strategy (for example, among others in `cartpole_swingup`, `insertion`, and `Robotank`) and failure (as in, for example, `manipulator_insert_ball`). For visualisation purposes, we use only 20 policies which are ordered by their ground truth returns (not observed by the method) and perfect predictions would be aligned along a diagonal line. We show the initial *OPE* values, current *selection* of the algorithm, *current* observation, past *observations* and the algorithm *prediction* with standard deviation for steps 1, 10, 50, and 100.
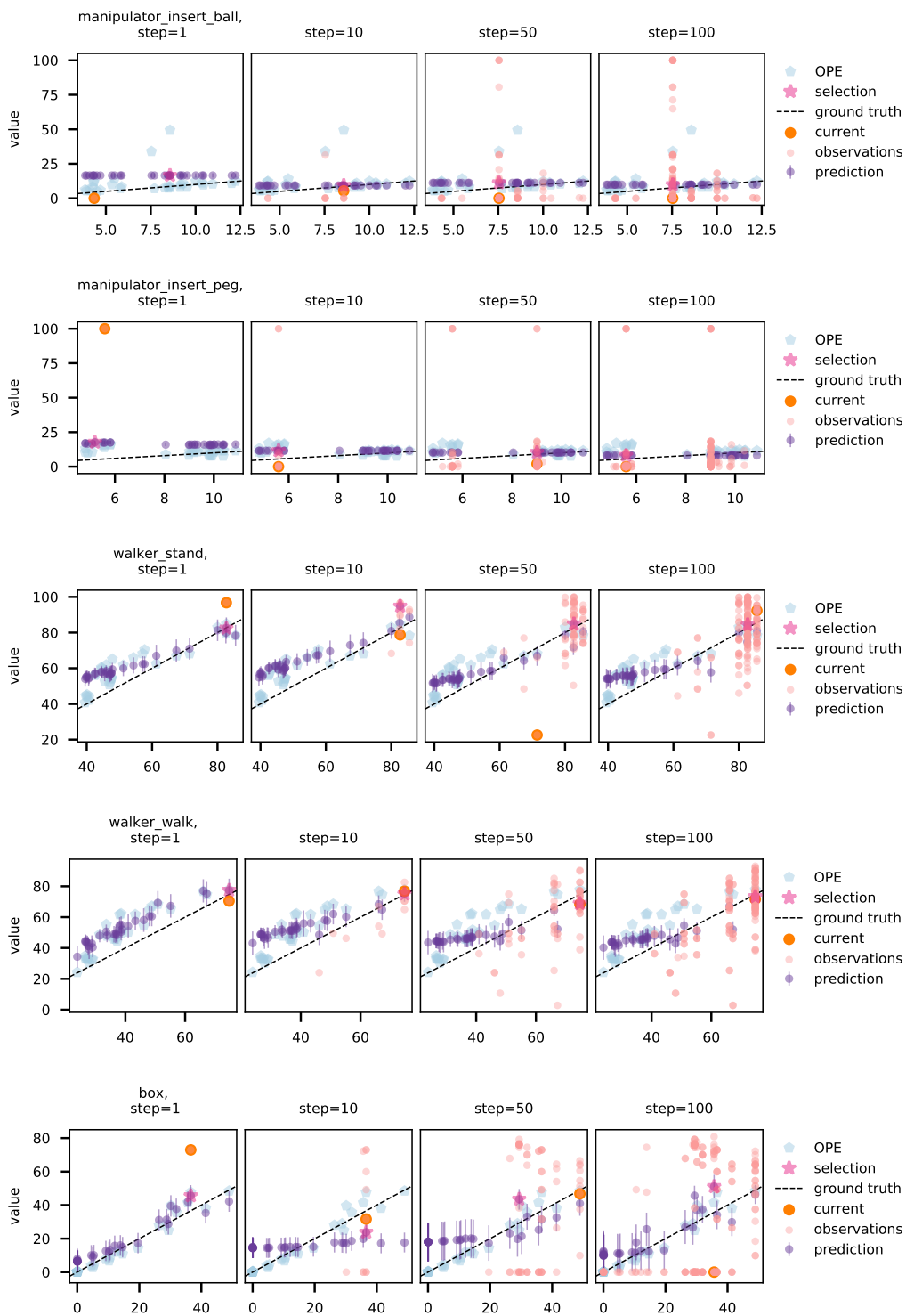
We can see that the initial selection is dominated by OPE prediction. Policy selection by OPE may be quite far from the best policy (for example, as in `manipulator_insert_ball`, `manipulator_insert_peg`, `insertion`, `slide`, Enduro), but it may also be very precise leaving no space for further improvement (for example, in `cheetah_run`, `walker_walk`). Notice that A-OPS prediction may be different from observations because our GP model assumes policies are correlated as defined by the policy kernel. An obvious example of this occurs at step $= 1$ when there are no online trajectories and only OPE scores are available. Intuitively, OPE scores are "smoothed" by the kernel when making a prediction. In practice it means that A-OPS predictions at the very few first interactions might be worse than OPE scores if OPE is highly accurate, but they rapidly improve as more online evaluations are collected and OPE is quickly outperformed. If we wanted to match the predictions of OPE at the very first iteration, we could perform the GP optimisation for many iterations and without any hyperparameter priors, but this would essentially result in overfitting and would not have any positive effect on the performance of our method with a moderate amount of online observations.
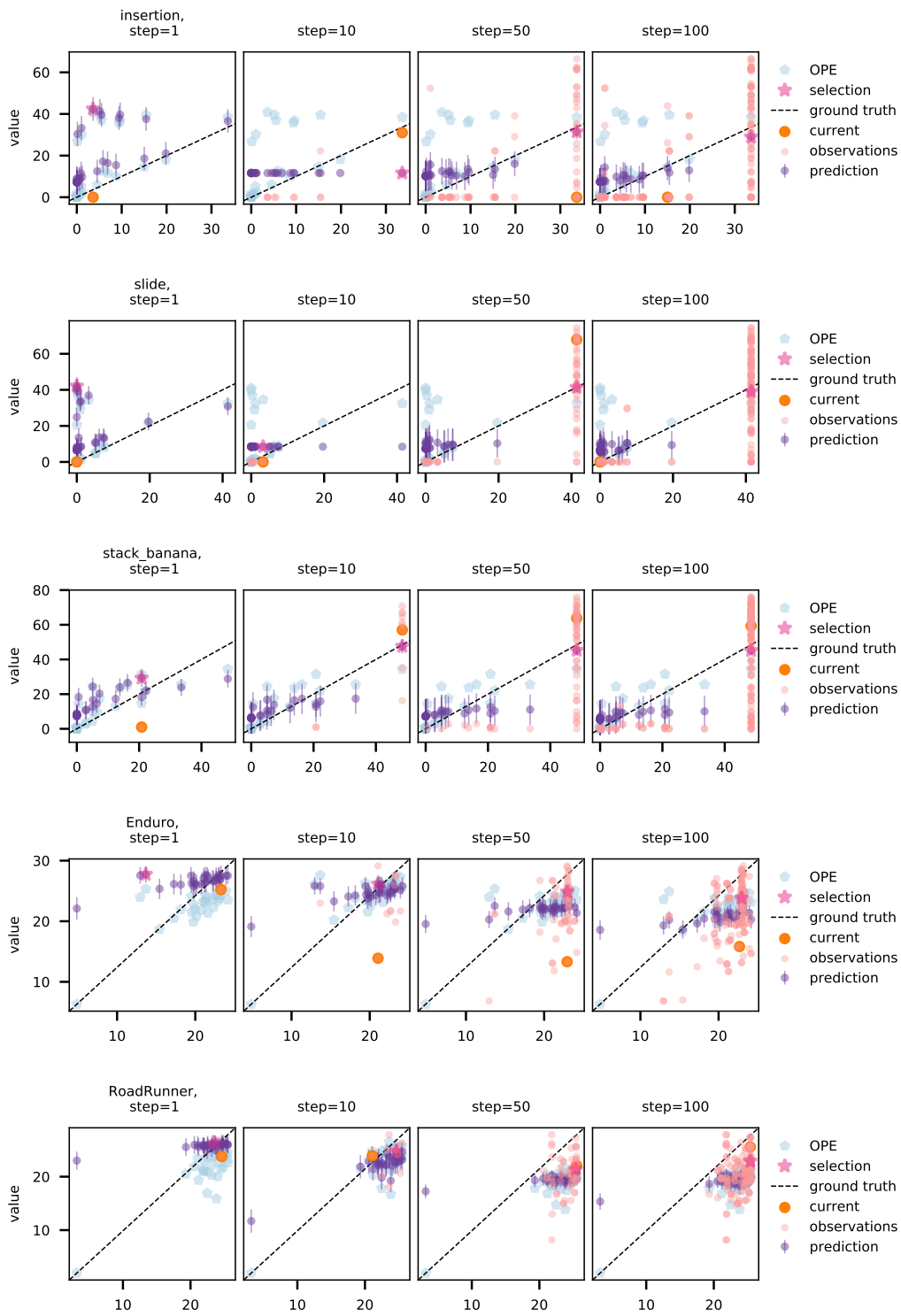
With more online observations, the prediction by A-OPS improves. We clearly see that the selected policies are not uniformly sampled and are biased toward more promising samples (there are usually more pink points towards the right of the figure). Furthermore, the predictions are interdependent, we can see that the predictions of the return of a particular policy might change even without any new observations of it.

In some experiments the visualisation shows that the predictions by the model are dominated by the variance of the episodic returns at some point during the training. For example, it happens in `cheetah_run`, `fish_swim`, `manipulator` tasks, and `insertion` when at some step during the trajectory acquisition, all predictions look rather "flat" as GP does not assign very different predictions to them given a small amount of observations, but with high variance.

In some experiments we do observe consistent overestimation (for example, in `cheetah_run`, `humanoid_run`, and `walker` tasks) and underestimation (for example, in Enduro and RoadRunner) by OPE methods. However, A-OPS method still performs well and is able to select a good policy for recommendation. It can recover quickly from this bias thanks to its kernel that brings policies with similar actions together: When a return is observed for one policy, the predictions for several related policies are adjusted automatically.
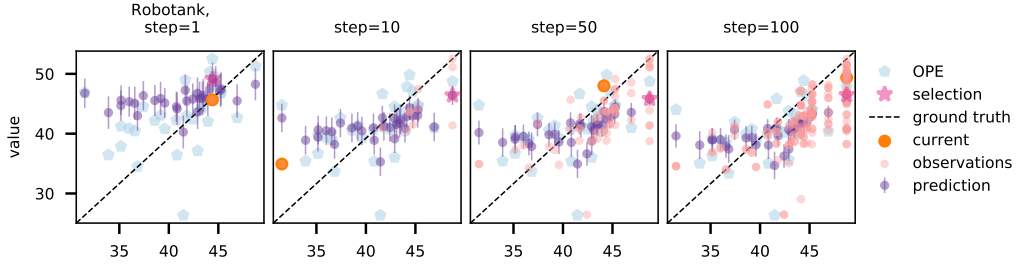
28

Figure 22: Visualisation of the qualitative performance of A-OPS algorithm on all the environments from dm-control, MPG and Atari domains with 20 randomly selected policies (ordered by ground truth only for the illustration purpose). From left to right we show the state at 1, 10, 50, 100 algorithm iterations. The initial OPE scores are shown in light blue, the policy selected by A-OPS is highlighted with a magenta star, the current observation by the algorithm is shown in orange circle, past observations are in pink and the prediction with its standard deviation is in purple.
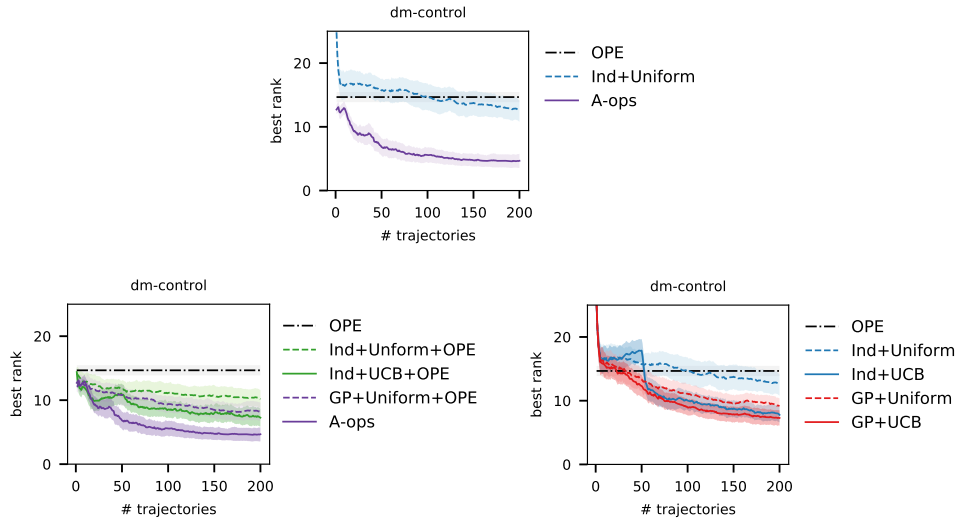

Figure 23: Ranking performance metric. Aggregated across 9 environments of the dm-control domain, we show the performance of the policy selection methods in terms of the rank of the selected policy. The same observations hold: A-OPS is the best strategy, active is better than uniform, methods that exploit policy correlation are better than methods that do not.

E   Additional experiments

Finally, in this section we present additional experiments that demonstrate various aspects of the problem and our proposed method.

E.1   Ranking as performance measure

We quantified the performance of the policy selection algorithms based on the simple regret so far. Other performance metrics could be used, for example, the rank of the selected policy. The best rank is 1 that means that the best policy was found and the worst rank is K, where K is the number of candidate policies. Fig. 23 shows results similar to Fig. 5 and Fig. 6 for the ranking metric. The same observations still hold.
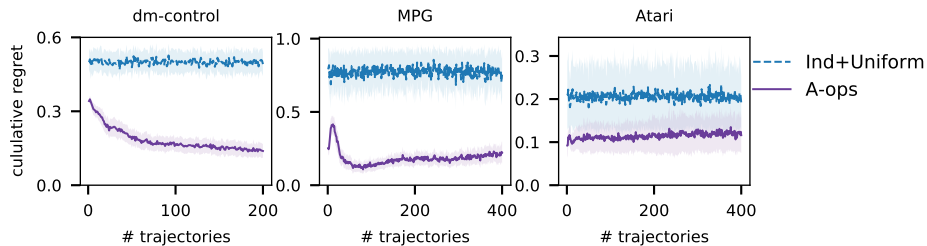
Figure 24: Cumulative regret of A-OPS is lower than that of online policy selection with IND+UNIFORM.

method	dm-control	MPG	Atari
	the worst policy		
IND+UNIFORM+OPE	2%	0.52%	0.52%
IND+UCB+OPE	1.2%	0.26%	0.31%
A-OPS	0.14%	0.007%	0.01%
	10% worst policies		
IND+UNIFORM+OPE	12%	10.6%	10.5%
IND+UCB+OPE	7.7%	5.4%	9%
A-OPS	1.3%	0.17%	1.4%

Table 6: The percentage of time that the worst and one of the 10% worst policies is executed during the policy selection procedure by different algorithms including A-OPS.

E.2   Cumulative and minimum regret

While the goal of A-OPS is to minimise the simple regret and not cumulative regret, it still avoids repetitive execution of most poorly performing policies when employing UCB criterion. As a result, A-OPS achieves lower cumulative regret than strategies based on uniform sampling as manifested by Fig. 24. Interestingly, towards the end of the experiment the cumulative regret starts growing slightly, that indicates that A-OPS goes back to the exploration phase again once a promising policy is identified.

We also analyse how often during the policy selection procedure A-OPS executes very bad policies. For this we compute the percentage of A-OPS (and alternative methods) iterations where the worst policy or one of the 10% worst policies is executed. Our findings are summarized in Tab. 6 for the three most representative algorithms. A-OPS strategy ends up querying the worst-performing policies significantly less frequently than other algorithms despite not being optimized for it directly. A potential explanation is that the policy kernel allows us to infer which policies are poorly performing in a very data efficient manner.

E.3   Varying amount of OPE estimated

Computing OPE estimates (like FQE or model-based OPE) can sometimes be expensive. Fig. 25 depicts the performance of A-OPS by providing OPE estimates for a random subset of $k \in [0, 50]$ policies in dm-control environment. Increasing the number of OPE observations consistently improves the results. This result demonstrates that our method A-OPS can seamlessly incorporate all the available information and benefit from the increasing number of initial observations.

E.4   Effect of the selections strategies

In the next experiment we study the effect of the choice of Bayesian Optimisation method on the performance of the A-OPS method. First, we investigate the influence of the exploration coefficient on the performance. It turns out that the performance of the A-OPS method is not very sensitive to the choice of exploration coefficient value. Our ablation study with various values in Fig. 26, right
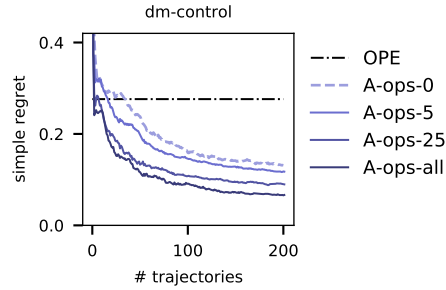
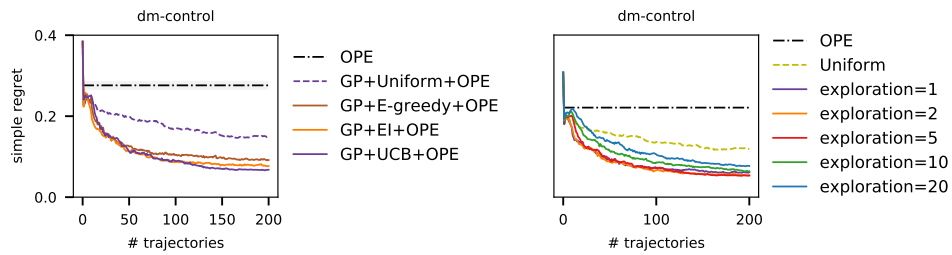Figure 25: The performance of A-OPS on dm-control with varying number of FQE

Figure 26: Left: The performance of A-OPS where different values of exploration coefficients are used. The difference between different coefficients is small for a wide range of values and using UCB criterion with any exploration value is better than doing uniform sampling. Right: The performance of various selection strategies in conjunction with GP+OPE in 9 environments of dm-control domain. The difference between uniform and active selection strategies is significant, while the difference between various active selection strategies is small. For better visualization, we do not show the standard deviation, which is comparable to the A-OPS result in Fig. 6.
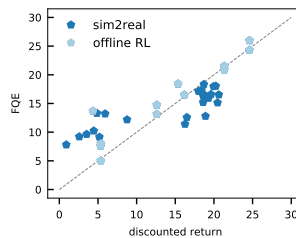

Figure 27: FQE results for sim2real (light blue) and offline RL (dark blue) policies. The correlation of FQE with the ground truth returns is very high.

shows that there is no difference in performance for the values between 1 and 7 and the performance slightly degrades, but still stays better than for the baselines, for the values 7-20.

Furthermore, we note that the selected best strategy A-OPS as GP+UCB+OPE is just one realisation of the active policy selection strategy. We chose UCB as our strategy as it demonstrated promising results across different environments and domains. However, other active selection strategies could be applied as well, for example, epsilon-greedy or expected improvement (EI). In Fig. 26, left we show the performance of various selection strategies in one domain. The choice of a BO strategy makes a considerably smaller difference than the increase of regret when using uniform sampling (GP+UNIFORM+OPE).

F   Real-world robotic experiments

For the real-world experiment with robotics data we performed OPE with FQE for the policies trained with sim2real and offline RL. To the best of our knowledge, this is the first time this method was applied to this domain. We present the results in Fig. 27 where the ground truth discounted return is plotted against the computed FQE values. The policies that were trained with sim2real approach are indicated with light blue and the policies trained on real world data are indicated in dark blue. We notice that all predicted FQE values are well correlated with the ground truth returns, the correlation coefficient is 0.842. There is no significant difference between the results of offlince policy evaluation with FQE for offline RL and sim2real policies and to the best of our knowledge this is the first demonstration of FQE for sim2real.